Volume: 1
Issue: 1
September, 2021

ADVANCED GEOMATICS

E-ISSN: 2791-8637

Advanced Geomatics

About Journal

The Advanced Geomatics Journal (AGE) covers all aspects and information on scientific and technical advances in the geomatics sciences. AGE publishes original and innovative contributions in geomatics applications ranging from the integration of instruments, methodologies, and technologies and their respective uses in the environmental sciences, engineering, and other natural sciences.
AGE is a double-blind peer-review journal. At least two reviewers, professionals in their field of specialization, evaluate the original article after the study was checked in iThenticate ® (Professional Plagiarism Prevention) software.

Aim & Scope

The scope of Advanced Geomatics;

- ✓ B All multidisciplinary studies with UAV
- ✓ Application of Geomatics
- ✓ Augmented Reality and Virtual Reality Applications with UAV
- ✓ Cartography
- ✓ Construction Surveys
- ✓ Crowdsourcing/volunteered geographic information
- ✓ Deformation and Landslide Measurements with UAV
- ✓ Deformation Measurements
- ✓ Digital Mapping
- ✓ Documentation Studies with UAV
- ✓ Geodesy
- ✓ Geodetic and Control Surveys
- ✓ Geographical Information Systems
- ✓ Geographical Information Systems Applications with UAV
- ✓ GNSS and GPS
- ✓ Hydrography
- ✓ Image Processing and Analysis
- ✓ Indoor navigation
- ✓ Industrial Measurements with UAV
- ✓ Land Information Systems (LIS)
- ✓ Mining Measurements with UAV
- ✓ Photogrammetry
- ✓ Positioning and navigation
- ✓ Precision Agriculture Practices with UAV
- ✓ Remote Sensing
- ✓ Sensors
- ✓ Spatial Data Analysis
- ✓ Spatial Information Science
- ✓ UAV LiDAR and Applications
- ✓ UAV Photogrammetry and Remote Sensing with UAV
- ✓ Urban Planning and Transportation Planning Studies with UAV

Publication frequency Biannual
WEB http://publish.mersin.edu.tr/index.php/geomatics/index
Contact myakar@mersin.edu.tr / aliulvi@mersin.edu.tr / ayasinyigit@mersin.edu.tr

Advanced Geomatics

Advanced Geomatics

Volume *1*

Issue *1* *September, 2021*

Contents

Research Articles;

Advanced Geomatics

http://publish.mersin.edu.tr/index.php/geomatics/index

e-ISSN: 2791-8637

The Analysis Methodology of Robotic Total Station Data for Determination of Structural Displacements

Hüseyin Pehlivan[*1]

[1]*Gebze Technical University, Faculty of Engineering, Department of Geomatics Engineering, Kocaeli, Turkey*

Keywords
Total station
Displacement
RTS
Deformation
Least Squares Method

ABSTRACT

Monitoring structural deformations and taking measures for building safety are considered almost synonymous with important concepts such as human health, public safety and prevention of economic losses. For this reason, new structural monitoring application techniques are being developed in parallel with the developments in building construction technologies and architecture. In particularly, GNSS satellite-based measurement systems have found wide application areas for determining structural oscillations and deformations. In addition, the direction of the studies in this field has focused on lower cost and more practical measurement systems. One of the alternative measurement devices used for this purpose is angle and distance measurements with the classical total station. Total stations, which have been automated and gained robotic features in recent years, are easily used in the determination of the most critical structural monitoring and deformations with their programmable structure. In this study, angle-distance measurements performed with a robotic total station at a simultaneous and constant sampling interval for 6 hours were processed and analyzed. Coordinate values and position errors were calculated by adjusting according to the least-squares method for each measuring range. Structural displacement values were determined from the coordinate values calculated as a function of time.

1. INTRODUCTION

In structural monitoring, electronic theodolites (ET) or total stations (TS) are commonly used to calculate the time-dependent changes of cartesian coordinates of observation points. These instruments are the most basic geodetic measuring instruments used in engineering measurements and scientific studies. Firstly, with the development of electronic theodolites, TSs emerged and later with automatized robotic total stations (RTS), which allow new generation robotic measurements, have found a wide area of use (Schofield and Breach 2007).

RTS or Robotic theodolites are a modern version of TS. In sampling intervals determined according to the features of the program used, RTS can direct itself to the target point, make measurements and record. Nowadays, by programming RTSs, it has been reached the level of observing with a sampling interval of 5-10 Hz and monitoring moving reflectors. Because of these advantages, it is widely used in many surveying and other engineering projects (Psimoulis and Stiros 2008; Psimoulis and Stiros 2011; Moschas et al. 2012; Lienarth et al. 2016). In addition to general engineering research, it can also be used in more scientific experiments to record oscillations with a high frequency greater than 1 Hz and small amplitude (a few mm). With this capacity, RTS have also be used for monitoring large engineering structures under the influence of wind or traffic load (Psimoulis and Stiros 2007; Pytharouli and Stiros 2008; Pehlivan 2009; Zhou et al. 2019). In addition, studies have been conducted in which they are used as auxiliary sensors in the determination of structural movements and deformations (Psimoulis and Stiros 2012, Pehlivan et. Al. 2013).

In this study, to determine the deformations of a tall structure, horizontal, vertical, and oblique distance measurements were made to model the building movements using total stations with robotic features from long distances. The data were processed and adjusted with the least-squares method to determine the position changes (structural deformations) of the observation point. Positional coordinates and position errors were calculated for each measuring moment, and time-dependent position changes were determined.

* **Corresponding Author**

*(hpehlivan@gtu.edu.tr) ORCID ID 0000-0002-0018-6912

Cite this article;

Pehlivan H (2021). The Analysis Methodology of Robotic Total Station Data for Determination of Structural Displacements: Advanced Geomatics, 1(1), 01-07

Research Article

Received: 03/09/2021; Accepted: 30/09/2021

2. MEASUREMENTS WITH TOTAL STATION

The RTS sends laser light to the prism mounted on the observed structure and can record the horizontal distance and the horizontal and zenith angles values using the round trip time of the returning light. Each observation record can be converted into coordinate values and its change over time helps us calculate the direction and trace of motion. Under normal atmospheric conditions, be making angle measurements with 0.5' and distance measurements with 1mm+1ppm accuracy allows us to determine the position with 1mm accuracy. Repeated measurements at regular intervals defined by a total station with automatic target recognition (ATR) system; It automatically performs the process of guiding to the target point, measuring and recording, as programmed. The speed of this automated measurement and recording process is directly proportional to the sampling rate of the measurement process (Psimoulis and Stiros 2011; Moschas et al. 2012; Pehlivan et al. 2013).

2.1. Measurements with Automatized Total Station or Robotic Total Station

Once the RTS is programmed, it automatically performs observations without the need for an operator and can save the data on a memory card. The data recorded during the measurement can be viewed in real-time if the RTS is connected to a computer. It provides instant monitoring of position changes, monitoring of displacement changes and a controlled test environment under loading conditions. These instant data are useful in eliminating system and human-induced errors in load and construction works. It also enables engineers in post-process processes to refine structural analysis or finite element model to examine general structural behavior and model dynamic response when necessary.

This dynamic response is closely related to the speed of change in the position of the observation point. Here, the measurement speed of TS, so data sampling recording rate, becomes important. RTS' target orientation, measurement and recording speeds give the total data sampling capacity of the instrument used. As the speed of these three features increases, it will be possible to monitor and record higher frequency dynamic behaviors. As the servo motor properties and software used to develop, it will be possible to monitor the movements even in vibration mode.

Distance and angle values from the observation point to the points to be measured can be measured automatically at certain intervals with RTS. Modern RTSs can measure the angle value with 0.5cc. While angle measurements in the range of 5-10cc can be performed with normal total stations, precise distance measurements can be performed with an accuracy of 0.1 mm and normal distance measurements with an accuracy of 1 mm. With this sampling range and measurement accuracy, RTS will continue to maintain its place as an indispensable measuring instrument in many engineering works as well as in many SHM (Structural Health Monitoring) works (Pehlivan 2019; Zhou et al. 2019).

2.2. Sources of Error in RTS

Total station measurements are affected by instrumental errors and external factors (changes in temperature, pressure and relative humidity). Although these sources of error affect the measurement accuracy, relative position changes can be determined and the direction and magnitude of the movement can be determined. Measurements can be performed with sufficient accuracy in building monitoring studies when instrument errors are minimized and corrections are brought to external factors. With an automated programmable TS, the accuracy of positioning depends on the measured angle and distance measurement accuracy. Angle and distance measurement may also vary depending on the distance made. The type of prism used in measurement may also cause deviations. And therefore it is important to use an appropriate prism depending on the purpose of the measurement.

3. DATA PROCESSING STRATEGY in DETERMINE STRUCTURAL DISPLACEMENTS

Different data processing strategies can be used depending on the expected type of movement in structural motion tracking studies. If slow deformation is expected at a constant rate, the data can be processed in static sessions from a few hours to several days, generally assuming no movement during the session. If the building movement or deformation in question does not pose an imminent threat to the structure or its surroundings or people living in the area, this is usually done after the procedure (Pehlivan 2009).

However, if the movement expected from the structure is expected to be "sudden deformation" for a short period of time and/or "continuous deformation" changes over time, the sampling interval should be increased accordingly. If the deformation could cause the deformed body to fail, a real-time solution is desired to detect the deformation as soon as it occurs and initiate the warning and evacuation processes. In the test study of this work, structural deformations are expected to have a slow character. In normal weather conditions, while the movement is slow, increasing impact loads such as temperature, wind, etc. will cause an increasing effect on the building movements. For these reasons, it is thought that in monitoring the constant and regular motion expected in normal atmospheric conditions, performing our observations with a few minutes sampling interval of RTS measurements will give us the opportunity to capture the expected movements. However, over a relatively short period of time, it can be preferred as a solution in real-time monitoring to detect movements of the structure.

3.1. Determining the Coordinates of the Monitored Point with the Least Squares Method

In the test measurements summarized in Figure 1, simultaneous observations were made at the same observation point (Prism P) by installing two automatic total station instruments at two fixed station points. Two lengths (oblique lengths) and two angle values

(horizontal and zenith angles) were recorded over six hours and at equal time intervals. As a function of time, zenith angles and oblique length measurements and horizontal distances S1 and S2 were calculated. Thus, horizontal angles (α1 and α2) and horizontal distances (S1 and S2) have been obtained as time series for each measuring epoch. The linear-angular intersection method was used to determine the coordinates and position accuracies of the P point with these data sets. This is because linear-angular intersection has the advantages of the least-squares method (Ehigiator et al. 2010; Okwuashi et al. 2014).

In these test measurements; the number of observations (S1, S2, α1, α2) is greater than the number of unknowns (Xp, Yp), and the least-squares method can be used to determine the coordinates of the P point. Thus, it is aimed to calculate the balanced coordinate values of the P point and to determine the displacement changes according to time by using the least-squares method. In this section, the formulas for determining the balanced coordinates of the P point by the least-squares method and calculating the displacements are given respectively.

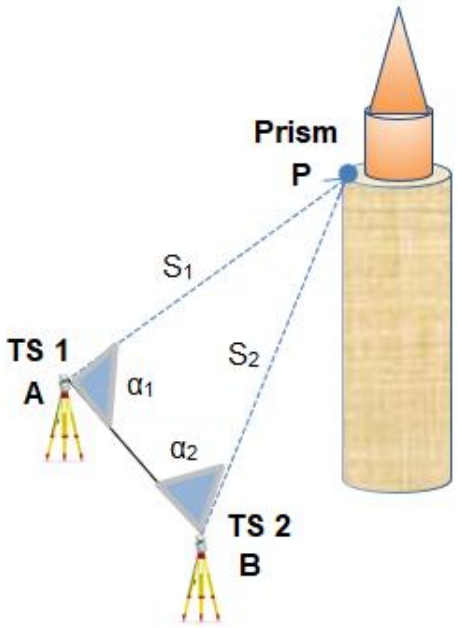

Figure 1. Test measurements and the geometry of angular-linear intersection.

All calculations were made with algorithms developed in the Matlab program. An adjusting model, which can be applied iteratively for each measurement epoch, has been applied in the triangle ABP formed by points A B and P. Since it is assumed that the weights of all measurements are equal, W = I is accepted.

Firstly; The approximate coordinates of the P point are calculated. The coordinates of point P are (Xp, Yp), the coordinates of fixed station points A and B are (XA, YA) and (XB, YB), respectively. The adjusting of these calculated coordinates was done by using the observation equation method. In this correction model (observational least square), the number of equations is equal to the number of observations (n = 4), each equation contains one observation and one or more unknowns. In this case, observations are S1, S2, α1, α2 and unknowns are Xp, Yp.

The two lengths (S1, S2) of the lines in the horizontal projection can be written in a coordinate form as follows:

$$S_1 = \sqrt{(X_P - X_A)^2 + (Y_P - Y_A)^2}$$

$$S_2 = \sqrt{(X_P - X_B)^2 + (Y_P - Y_B)^2} \quad (1)$$

The horizontal angles (α_1 and α_2) from figure 1 can be calculated as follows:

$$\alpha_1 = cos^{-1}\left(\frac{\overline{AP}^2+\overline{AB}^2-\overline{PB}^2}{2\,\overline{AP}\,\overline{AB}}\right)$$

$$\alpha_2 = cos^{-1}\left(\frac{\overline{BA}^2+\overline{BP}^2-\overline{AP}^2}{2\,\overline{BA}\,\overline{BP}}\right) \quad (2)$$

Using the coordinates of the points, we can write equations 2 as follows:

$$\alpha_1 = cos^{-1}\left[\frac{(X_P-X_A)^2+(Y_P-Y_A)^2+AB^2-(X_P-X_B)^2+(Y_P-Y_B)^2}{2\,AB\,\sqrt{(X_P-X_A)^2+(Y_P-Y_A)^2}}\right]$$

$$\alpha_2 = cos^{-1}\left[\frac{(X_P-X_B)^2+(Y_P-Y_B)^2+\overline{AB}^2-(X_P-X_A)^2+(Y_P-Y_A)^2}{2\,\overline{AB}\,\sqrt{(X_P-X_B)^2+(Y_P-Y_B)^2}}\right] \quad (3)$$

The four observational equations given in equations 1 and 3 are nonlinear functions of both parameters and observations; they can be processed by the least-squares adjustment technique. Before starting the solution, approximate values of unknown parameters are calculated. Approximate values of the coordinates of the P point are calculated using the angular intersection according to the following formulas (Ehigiator 2005, Ehigiator et al. 2010):

$$X_P^0 = \frac{X_A\,cot\,\alpha_2+X_B\,cot\,\alpha_1-Y_A+Y_B}{cot\,\alpha_1+cot\,\alpha_2}$$

$$Y_P^0 = \frac{Y_A\,cot\,\alpha_2+Y_B\,cot\,\alpha_1-X_A+X_B}{cot\,\alpha_1+cot\,\alpha_2} \quad (4)$$

Using these X_P and Y_P values, the approximate values of the observation equations (Lo) are calculated. Then the misclosure vector (L) is calculated as:

$$L = L^0 - L_{abs} \quad (5)$$

We can express the linearized model in matrix form as follows:

$$V_{4\times1} = A_{4\times2} \,.\, X_{2\times1} + L_{4\times1} \quad (6)$$

Where; A: the coefficients matrix of parameters, L: the misclosure vector, V: the residuals vector. Matrix A may be computed by differentiation of the four equations with respect to the two unknowns and can be written in the form:

$$A_{(4\times2)} = \begin{bmatrix} \frac{\partial S_1}{\partial X_P} & \frac{\partial S_1}{\partial Y_P} \\ \frac{\partial S_2}{\partial X_P} & \frac{\partial S_2}{\partial Y_P} \\ \frac{\partial \alpha_1}{\partial X_P} & \frac{\partial \alpha_1}{\partial Y_P} \\ \frac{\partial \alpha_2}{\partial X_P} & \frac{\partial \alpha_2}{\partial Y_P} \end{bmatrix} \quad (7)$$

With the Matlab program, the elements of the matrix A (a_{ij}) can be found by differentiating the four observation equations. Then the normal equation system is written like this:

$$N_{2\times2} \; . \; \hat{X}_{2\times1} + U_{2\times1} = 0 \quad (8)$$

Where,

$$N_{2\times2} = A^T_{2\times4} \; . \; W_{4\times4} \; . \; A_{4\times2} \quad (9)$$

And,

$$U_{2\times1} = A^T_{2\times4} \; . \; W_{4\times4} \; . \; L_{4\times1} \quad (10)$$

The solution for the normal equation system (8) is as follows;

$$\hat{X}_{2\times1} = -N^{-1}_{2\times2} \; . \; U_{2\times1} \quad (11)$$

After this, the adjusted unknown parameters can be estimated as follows:

$$\bar{X}_{2\times1} = \hat{X}_{2\times1} + X^0_{2\times1} \quad (12)$$

The vector of adjusted observations can be estimated as follow:

$$\bar{L}_{4\times1} = \hat{V}_{4\times1} + L_{4\times1} \quad (13)$$

The estimated variance factor is:

$$\sigma_0^2 = \frac{v^T.W.V}{r} = \frac{v^T.W.V}{2} \quad (14)$$

The estimated variance-covariance matrix of the parameters is as follows:

$$C_X = \sigma_0^2 \; . N^{-1} \quad (15)$$

And as a result, the variance-covariance matrix of adjusted observations are computed follow as:

$$C_L = A \; . \; C_X \; . \; A^T \quad (16)$$

Like the other operations above, this normal equation (16) can be solved using the Matlab program too. The positional error at point P can be calculated using the following equation (Allan 1988):

$$M_P = \frac{b \; m''_\alpha}{\rho'' \sin\gamma} \sqrt{sin^2_{\alpha_1} + sin^2_{\alpha_2}} \quad (17)$$

Where; b: base line (the distance between total stations) (b=AB length in figure 1); m_α'': mean square error of measured horizontal angles (taken from specifications of the used total stations); α_1: the horizontal angle at point A, α_2: the horizontal angle at point B, γ: the horizontal angle at point P and ρ''=206265 "from the small angle formula" (Ehigiator et al. 2010).

In order to accept the observations of the point P from the triangle ABP and its adjusted coordinates to be sufficiently accurate, the coordinates must satisfy the following condition (Ashraf 2010).

$$r_P = \sqrt{\Delta_x^2 + \Delta_y^2} \leq 3 \; M_t \quad (18)$$

Where;

$\Delta_X = X_i^P - X_k^P$, $\Delta_Y = Y_i^P - Y_k^P$ ve $M_t = \sqrt{M_i^2 - M_k^2}$,

X_i^P , Y_k^P: the adjusted coordinates of the point P at the time i of measurement; X_i^P, Y_k^P: the adjusted coordinates of the point P at the time k of measurement; M_i and M_k : the position errors of the point P at the time i and k of measurement (Ashraf 2010).

3.2. Determining the displacement vectors of the observed point

If we consider the position changes in 2 dimensions, let's assume that two coordinate values x_i,y_i and x_k,y_k are recorded at an observation point at times i and k. The displacements of the observation point between the time i and k will be dn (Δx, Δy).
The coordinate displacements from the coordinates obtained at time i and k in the time interval $\Delta_t = t_k - t_i$;

$\Delta x = x_k - x_i$, displacement on the x-axis
$\Delta y = y_k - y_i$, displacement on the y-axis
$\Delta t = t_k - t_i$, time difference between measurements.

Expressed as the coordinate differences of point displacements, each of Δx, Δy denotes a motion vector. And and each of them has a magnitude and direction. Collectively, these vectors define the field of displacement in a given time interval.
Comparison of the magnitude of the calculated displacement and the associated measurement accuracy indicates whether the detected motion is more likely due to measurement error:

$$| dn | < (pn) \quad (19)$$

Where; dn is the magnitude of the displacement (for point n), (pn) = maximum size of the combined 95% confidence ellipse for point n = (1.96).

$pn = \sqrt{\sigma f^2 + \sigma i^2}$ and σf (next) or standard error in position for the last measurement, σi (previous) or standard error in position for reference measurement.

4. EVALUATION of EXPERIMENTAL TESTS RESULTS

Test data were collected with the measuring setup given in Figure 1 using two automatized total stations installed at points A and B. Horizontal-zenith angle observations and oblique distance measurements, from points A and B whose coordinates are known to the monitoring point P on the tower, was recorded with a measurement recording period of 2 minutes. The data sets obtained as time series were pre-audited and each observation data set was inspected within itself. The time series consisting of 2 angles and 2 lengths were resampled with a sampling interval of 30 minutes. In other words, 30-minute new data sets were created by taking the average of 15 measurement values recorded every 30 minutes. Thus, it was aimed to determine the change of total displacement according to time with the observation sets created during the measurement period and providing also ease of operation.

For this purpose, adjusted coordinate values (Xp, Yp) and position errors (Mp: equation 17) of the observation point P were calculated for each half-hour time between 11:00 and 17:00 using the least-squares equations model (given in section 3.1). The adjusted coordinates calculated from the observations obtained during the observation period are presented in Table 1. Measurements that started at 11 o'clock were completed at 17:00 and coordinate values were calculated every 30 minutes. Since the position errors for each epoch depend on approximately the same parameters, approximately the same values were calculated (Mp=∓3.825 mm).

To test the accuracy of the adjusted coordinate values; The rp and Mt values given in equation 18 were calculated using the position errors calculated for each measurement period of the P point (Mt= 5.41 and 3*Mt= 16.23). As a result of the comparison and evaluation; It has been accepted that the observations made to point P in triangle ABP and its adjusted coordinates are sufficiently accurate. The corrected coordinates calculated from the data recorded during the observation period and their accuracy test results are presented in Table 1. The measurements that started at 11 o'clock were completed at 17:00 and the raw and corrected coordinate values calculated every 30 minutes and the differences between them are shown in Table 1.

Table 1. The adjusted coordinates and position errors of the observed point P

Time	$X_{adjusted}$	X_{raw}	$Y_{adjusted}$	Y_{raw}	dx	dy	$r_P \leq 3 * M_t$
11:00	914.2165	914.2132	449.4410	449.4440	-3.30	3.00	4.46
11:30	914.2163	914.2129	449.4381	449.4430	-3.40	4.90	5.97
12:00	914.2162	914.2123	449.4350	449.4364	-3.90	1.40	4.14
12:30	914.2162	914.2119	449.4324	449.4303	-4.30	-2.10	4.79
13:00	914.2159	914.2107	449.4311	449.4272	-5.20	-3.90	6.50
13:30	914.2161	914.2116	449.4297	449.4239	-4.50	-5.80	7.34
14.00	914.2174	914.2172	449.4297	449.4242	-0.20	-5.50	5.50
14:30	914.2171	914.2162	449.4302	449.4257	-0.90	-4.50	4.59
15:00	914.2170	914.2154	449.4314	449.4282	-1.60	-3.20	3.58
15:30	914.2182	914.2203	449.4336	449.4328	2.10	-0.80	2.25
16:00	914.2189	914.2232	449.4373	449.4407	4.30	3.40	5.48
16:30	914.2200	914.2280	449.4390	449.4454	7.99	6.40	10.24
17:00	914.2204	914.2299	449.4408	449.4494	9.57	8.60	12.87

In order to determine the structural displacements between the data that passed the accuracy-test and the measurement epochs, the coordinate differences for the periodic times were calculated separately for the X and Y directions (Table 2). The magnitude of the displacement (dn) at each periodic n point was calculated and tested by equation 19 and the results are presented in Table 2. According to Table 2, the displacements between the measurement epochs remained within the 95% confidence ellipse in magnitude. The displacements of the P point in the X and Y directions are presented in Figure 2. Accordingly, the total is the magnitude of the displacement from the adjusted coordinates of the P observation point were calculated as 24.60 mm. According to these calculated results, it has been determined that the structural displacement was approximately 2.5 cm from the six-hour measurements performed with the RTS. The representation of position changes with respect to time on the X/Y plane is presented in Figure 3.

Table 2. Displacement magnitudes of the observation point P

Time	Δx (mm)	Δy (mm)	|dn| < (pn=16.23)
11:30	-0.25	-2.90	2.91
12:00	-0.13	-3.19	3.19
12:30	-0.07	-2.57	2.57
13:00	-0.28	-1.28	1.31
13:30	0.23	-1.458	1.47
14.00	1.29	0.09	1.29
14:30	-0.29	0.43	0.52
15:00	-0.16	1.19	1.20
15:30	1.21	2.20	2.50
16:00	0.75	3.71	3.79
16:30	1.06	1.76	2.06
17:00	0.46	1.74	1.80

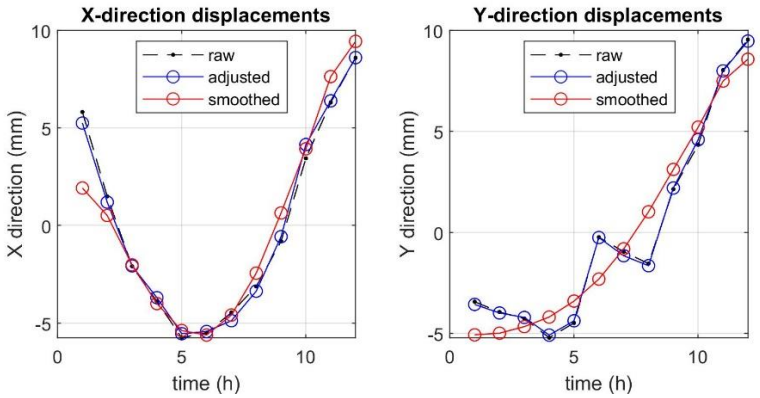

Figure 2. Displacements in X and Y directions with recorded raw data, adjusted and corrected coordinates.

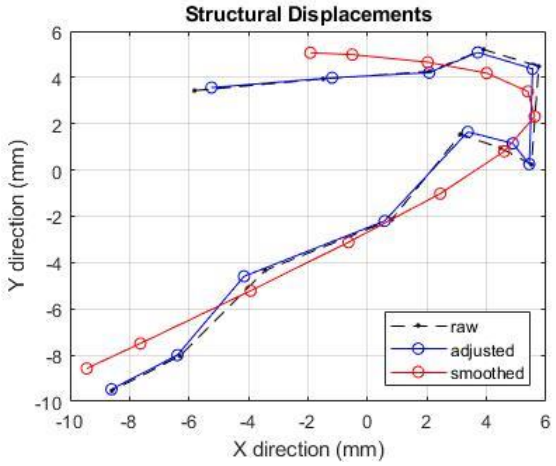

Figure 3. For observation point P, plotted positional displacements with recorded raw data, adjusted and corrected coordinates.

5. CONCLUSION

Continuous or periodic monitoring of buildings and determining their deformation characteristics will provide an important foresight for building health and life safety. Achieving the desired performance in structural monitoring depends on the use of correct measurement systems and correct analysis methods. It is a known fact that incorrect analysis of measurement data prevents some deformations from being noticed. The monitoring period and the most appropriate measurement system should be selected, taking into account the structural features, and should be evaluated with the most appropriate analysis methods.

Total stations with robotic features are proven instruments in structural deformation measurements. Although it has some handicaps during measurement, it is one of the first devices that comes to mind in structural deformation studies due to its measurement precision and practical measurement possibilities. The analysis process of the data recorded with RTS is also an important issue in order to make an accurate deformation estimation.

Within the scope of this study, structural monitoring data recorded for 6 hours under normal meteorological conditions were analyzed. The displacement vectors of each measurement time were calculated by calculating the coordinate values and mean errors balanced by the least-squares method. As a result of analysis and evaluation; It was concluded that the movement of the structure was within the known and predicted limits and the measurements were made with sufficient accuracy

Author contributions

All contributions belong to the author in this paper.

Conflicts of interest

The author declare no conflicts of interest.

Statement of Research and Publication Ethics

The author declare that this study complies with Research and Publication Ethics

REFERENCES

Allan A L (1988). The Principles of Theodolite Intersection Systems A. L. Allan Survey Review. 226-234.

Ashraf A B (2010). Development and Innovationof Technologies for Deformation Monitoring of Engineering Structures Using Highly Accurate Modern Surveying Techniques and Instruments, Ph.D. thesis, Siberian State Academy of geodesy SSGA, Novosibirsk, Russia, 205 p. [Russian language].

Ehigiator-Irughe R (2005). Environmental safety and monitoring of crude oil storage tanks at the Forcados terminal. M.Eng Thesis, Department of çivil Engineering, university of Benin, Benin City. Nigeria.

Ehigiator-Irughe R, Ehiorobo J O & Ehigiator M O 2010. Distortion of oil and Gas infrastructure from Geomatics support view, Journal of Emerging Trends in Engineering and Applied Sciences (JETEAS) Vol 1 (2010) 14-23 Toronto, Canada.

Lienhart W, Ehrhart M & Grick M (2016). High frequent total station measurements for the monitoring of bridge vibrations, J. Appl. Geodesy 2017; 11(1): 1–8, DOI 10.1515.

Moschas F, Psimoulis P & Stiros S (2012). GPS-RTS data fusion to overcome signal deficiencies in certain bridge dynamic monitoring projects, Smart Structures and Systems, Vol. 12, No. 3-4 (2013) 251-269.

Pehlivan H, Aydin Ö, Gülal E & Bilgili E (2013). Determining the behaviour of high-rise structures with geodetic hybrid sensors. Geomatics Nat Hazard Risk. doi:10.1080/19475705.2013.854280

Pehlivan H (2009). The Investigation of Dynamic Behaviors in Structures With Real-Time Kinematic GPS, PhD Thesis, Yildiz Technical University, Istanbul, (in Turkish).

Pehlivan H (2019). Robotik Total Station ve GNSS Ölçümlerinin Analizi. Erzincan University Journal of Science and Technology 2019, 12(2), 1018-1027 ISSN: 1307-9085. DOI: 10.18185/erzifbed.541895

Psimoulis P & Stiros S (2007). Measurement of deflections and of oscillation frequencies of engineering structures using Robotic Theodolites (RTS), Engineering Structures, 29 (12), 3312-3324, 2007.

Psimoulis P & Stiros S (2008). Experimental assessment of the accuracy of GPS and RTS for the determination of the parameters of oscillation of major structures. Computer-Aided Civil and Infrastructure Engineering, 23, 389-403.

Psimoulis P & Stiros S (2011). Robotic Theodolites (RTS) Measuring Structure Excitation. GIM International, 25(4), 29-33.

Psimoulis P and Stiros S (2012). A supervised learning computer-based algorithm to derive the amplitude of oscillations of structures using noisy GPS and Robotic Theodolites (RTS) records, Comput. Struct., 92-93, 337-348.

Pytharouli S & Stiros S (2008). Spectral Analysis of Unevenly Spaced or Discontinuous Data Using the 'Normperiod' Code, Computers and Structures, 86(1-2), pp190-196.

Schofield W and Breach M (2007). Engineering Surveying. UK. Elsevier Ltd., 2007. 622 pp. ISBN 978-0-7506-6948-8.

Okwuashi O and Asuquo I (2014). Basics of Least Squares Adjustment Computation in Surveying. International Journal of Science and Research (IJSR). Volume 3 Issue 8, ISSN (Online): 2319-7064.

Zhou J, Xiao H, Jiang W, Bai W & Liu G (2019). Automatic subway tunnel displacement monitoring using robotic total station, Measurement, Measurement, Volume 151, article id. 107251. https://doi.org/10.1016/j.measurement.2019.107251

Advanced Geomatics

http://publish.mersin.edu.tr/index.php/geomatics/index

e-ISSN: 2791-8637

Calculation of Centering Elements by Methods Other Than the Classical Method

Fazlı Engin Tombuş[1], Yener Türen[2], Nuri Erdem*[3], Hüseyin İnce[1]

[1]*Hitit University, Vocational School of Technical Sciences / Department of Architecture and City Planning, Çorum, Turkey*
[2]*Trakya University, Vocational School of Technical Sciences / Department of Architecture and City Planning, Edirne, Turkey*
[3]*Osmaniye Korkut Ata University, Faculty of Engineering, Department of Geomatics Engineering, Osmaniye, Turkey*

Keywords
Centering elements,
Reduction of off-center observations to the center,
Calculation of centering elements,

ABSTRACT

In cartography, when it is necessary to measure the angle at the center of the minaret, on which no tools can be installed, a point marked on the minaret balcony is used as the off-center point. The calculation of the basic elements required to reduce the angle measurements made at this off-center point to the center point is called "Calculation of Centering Elements". In the local coordinate system created with the help of two points established on the land near the minaret in the classical method, the centering elements can be calculated after the coordinates of the center point and the off-center point are found. It is possible to calculate the centering elements with other methods besides the classical method. As a matter of fact, there is also a study in the past that provides convenience in calculation. In this study; taking into account the other study on this subject, another method that does not require coordinate calculation is explained. Numerical applications related to the subject have been made in such a way as to reset the effects of rounding errors. The results obtained with other methods and the classical method were examined. At the end of the study, the findings and opinions are stated.

1. INTRODUCTION

In cartography, when it is necessary to measure the angle at the center of the minaret, on which no tools can be installed, a point marked on the minaret balcony is used as the off-center point. The calculation of the basic elements required to reduce the angle measurements made at this off-center point to the center point is called "Calculation of Centering Elements". In order to reduce the measurements made at the off-center point to the center point, the so-called centering elements must be calculated. In order to make this calculation, two auxiliary points (A, B) are established on the ground near the minaret (Figure 1).

In the classical method, a local coordinate system is created with the help of these points, one of these points is accepted as the starting point, and the coordinates of the center point (Z) and the off-center point (D) are calculated. After these calculations, the centering elements (DZ=e, αZ) are calculated. Instead of this method, which requires a long calculation process, another method has been developed that provides convenience in the past (Allan et al. 1968; Kıran 1983). Today, it is possible to calculate the centering elements by another method.

In this study; Taking into account the other study on this subject, another method that does not require coordinate calculation is explained (Figure 2). Practices related to the subject were made, and the findings and opinions obtained as a result of the study were stated.

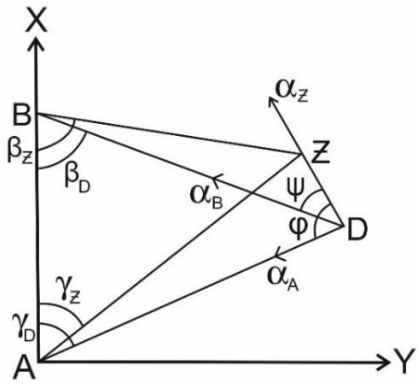

Figure 1. Centering elements according to the classical method

* **Corresponding Author**

(fengintombus@hitit.edu.tr) ORCID ID 0000-0002-2607-3211
(yenerturen@trakya.edu.tr) ORCID ID 0000-0003-3381-3780
*(nurierdem@osmaniye.edu.tr) ORCID ID 0000-0002-1850-4616
(huseyinince@hitit.edu.tr) ORCID ID 0000-0001-6118-5502

Cite this article;

Tombuş F E, Türen Y, Erdem N & İnce H (2021). Calculation of Centering Elements by Methods Other Than the Classical Method. Advanced Geomatics, 1(1), 08-13

Research Article

Received: 04/09/2021; Accepted: 29/09/2021

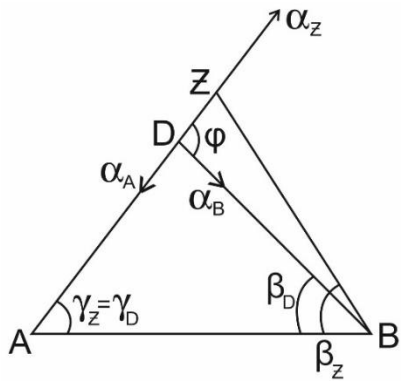

Figure 2. According to the first method centering elements

2. CALCULATION METHODS of CENTERING ELEMENTS OTHER THAN the CLASSICAL METHOD

2.1. First Method

The basis of this method is to mark the off-center point on the minaret balcony on the direction connecting the auxiliary point on the ground to the central point (Kıran 1983; Wolf and Ghilani 2008).

In Figure 2;
Z: The center point in the minaret realm,
D: The off-center point marked on the minaret balcony,
A and B: Auxiliary points marked on the land near the minaret,
DZ=e, αz : Indicates the centering elements.
Angles Z =D, βZ, βD and edge AB are measured from points A and B in the field.
In addition, horizontal distances AD and BD can be measured with an electronic tachometer.

From Figure 2, angle φ and sides AZ, BZ and DZ in triangle AZB are obtained from the following relations.

$$\varphi=\gamma_Z+\beta_D \quad (1)$$

$$AZ=\frac{AB*sin\beta Z,}{\sin(\gamma_{Z+\beta_Z})} \quad (2)$$

$$BZ=\frac{AB*sin\delta Z,}{\sin(\gamma_{Z+\beta_Z})} \quad (3)$$

$$DZ=AZ-AD \quad (4)$$

Since the direction measurements are made from the D point to the surrounding triangulation points, A and B points, the unknown αz is obtained from the following relations (Kıran 1983).

$$\alpha_z=\alpha_A+200 \quad (5)$$

$$\alpha_z=\alpha_B-\varphi \quad (6)$$

To make this method even easier, the following application can be made. With the electronic tachometer instruments produced today, it is possible to orientate from one point to another with a certain directional angle (URL_1). By making use of this feature of the instrument, if the direction angle of αA =200.0000 is viewed as the direction angle to point A while observing point A from the off-center point D, then the direction angle of the Z center point becomes αz=0.0000. Relation (6) is used as a control.

After obtaining the αz and DZ centering elements, the rules specified in the reduction of off-centre observations to the center are applied to reduce the angles measured at the D point to the Z point. (Atasoy 2014; Aydın 1974; İnce et al. 2021; Uren and Price 1986; Özbenli and Tüdeş 1989; Şerbetçi and Atasoy 2000).

2.2. Second Method

The basis of this method is calculating the centering elements from the triangles formed by tangent and cosine relations without making coordinate calculations. By making observations from the auxiliary point A to the points B, Z, D, the angles Z, D and the edge AB are measured. βZ, βD angles are measured by observing from auxiliary point B to points Z, D, A. The sides of AZ, AD, BZ, BD are obtained from the following equations by applying the sine relation in triangles ABZ and ABD (Figure 3).

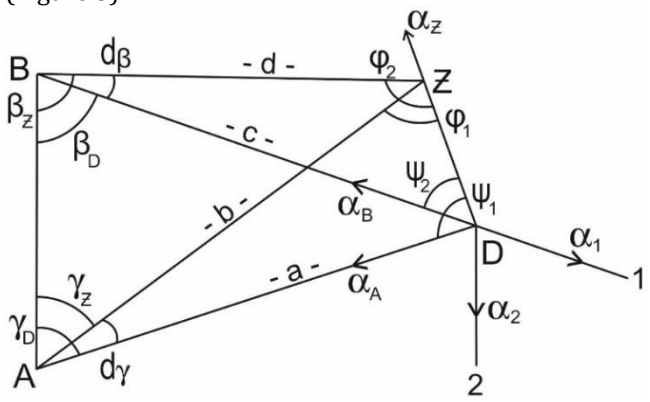

Figure 3. Observations from the auxiliary point A and B to the points B, Z, D

$$AZ=\frac{AB*sin\beta Z,}{\sin(\gamma_{Z+\beta_Z})} \quad (7)$$

$$BZ=\frac{AB*sin\gamma_Z,}{\sin(\gamma_{Z+\beta_Z})} \quad (8)$$

$$AD=\frac{AB*sin\beta D,}{\sin(\beta_D+\gamma_D)} \quad (9)$$

$$BD=\frac{AB*sin\delta D,}{\sin(\beta_D+\gamma_D)} \quad (10)$$

In Figure 3, a=AD, b=AZ, c=BZ, d=BD, dγ=γD -γZ, dβ= βZ – βD are abbreviated. In triangles AZD and BZD, the cosine relation for DZ is written.

$$DZ=\sqrt{(a^2+b^2-2*a*b*cosd\gamma)} \quad (11)$$

$$DZ=\sqrt{(c^2+d-2*c*d*cosd\beta)} \quad (12)$$

In Figure 3, the following relation is written for $\frac{\varphi_1+\psi_1}{2}$ in triangle AZD

$$\frac{\varphi_1+\psi_1}{2} = \frac{200-d\gamma}{2} \quad (13)$$

and the tangent relation for $\frac{\varphi_1-\psi_1}{2}$ is written.

$$\frac{\varphi_1-\psi_1}{2} = arc\tan((a-b)*\tan(\frac{\varphi_1+\psi_1}{2})/(a+b) \quad (14)$$

Considering equations (13) and (14), φ_1 and ψ_1 are obtained from the following relations.

$$\varphi_1 = \frac{\varphi_1+\psi_1}{2} + \frac{\varphi_1-\psi_1}{2} \quad (15)$$

$$\psi_1 = \frac{\varphi_1+\psi_1}{2} - \frac{\varphi_1-\psi_1}{2} \quad (16)$$

Similarly, in Figure 3, the following equations are written for $\frac{\varphi_2+\psi_2}{2}$ and $\frac{\varphi_2-\psi_2}{2}$ in triangle BZD.

$$\frac{\varphi_2+\psi_2}{2} = \frac{200-d\beta}{2} \quad (17)$$

$$\frac{\varphi_2-\psi_2}{2} = arc\tan((c-d)*\tan(\frac{\varphi_2+\psi_2}{2})/(c+d) \quad (18)$$

Considering the equations (17) and (18), φ_2 and ψ_2 are obtained from the following relations.

$$\varphi_2 = \frac{\varphi_2+\psi_2}{2} + \frac{\varphi_2-\psi_2}{2} \quad (19)$$

$$\psi_2 = \frac{\varphi_2+\psi_2}{2} - \frac{\varphi_2-\psi_2}{2} \quad (20)$$

Considering the direction angles α_A and α_B in Figure 3, α_Z is obtained from the following equations.

$$\alpha_Z = \alpha_A + \varphi_1 \quad (21)$$

$$\alpha_Z = \alpha_B + \varphi_2 \quad (22)$$

As can be seen, the centering elements were calculated with the above-mentioned relations without creating a local coordinate system.

3. NUMERICAL APPLICATIONS

Here, one numerical application was made for the first method and two numerical applications were made for the second method and classical method.

In the calculations made with the classical method and the second method, the fraction of the integer is taken up to the eighth digit after the comma in order to eliminate the effect of the rounding error on the results (Yüncü and Aslan 2002; Dilaver 2010).

3.1. Numerical Application 1

In accordance with Figure 2, calculate the centering elements with the first method, taking into account the measurements made at points A, B and D given in Table 1.

Table 1. Measurements made at points A, B and D

Station Point	Point of View	Horizontal Angle	Horizontal Distance	Station Point	Point of View	Horizontal Angle	Horizontal Distance
A	Z	0.0000		D	1	0.0000	
	D	0.0000	52.535		2	127.3356	
	B	83.3236	50.138		…		
B	A	0.0000	50.137		B	242.6565	
	D	60.2750	62.526		A	299.3580	
	Z	61.3632					

Solution:

$\gamma=\gamma_Z=\gamma_D$=83.3236, β_D =60.2750, β_Z=61.3632, AB=50.138 m, α_A=299.3580, α_B=242.6565

$\varphi=\gamma+\beta_D$=143.5986, ψ=200-($\gamma+\beta_Z$)=55^g.3132

AZ=$\frac{AB*sin\beta Z,}{\sin\psi}$=53.935 m e=AZ-AD=1.40 m

$\alpha_z = \alpha_A$ +200-400=99.3580, $\alpha_z = \alpha_B - \varphi$=99.3579,

Average value α_z =99.3580

3.2. Numerical Application 2

Calculate the centering elements with the classical method and the second method, taking into account the measurements made at points A, B and D given in Table 2, in accordance with Figure 1 and Figure 3.

Table 2. Measurements made at points A, B and D

Station Point	Point of View	Horizontal Angle	Horizontal Distance	Station Point	Point of View	Horizontal Angle	Horizontal Distance
A	B	0.0000	94.376	D	1	0.0000	
	Z	71.8280			2	127.3356	
	D	75.4420			…		
B	Z	0.0000			A	161.3819	
	D	1.1820			B	244.7059	
	A	42.4140	94.376				

Obtaining and simply balancing the elements to be used in the calculations:

γ_Z=71^g.8280, γ_D=75^g.4420, β_D=41^g.2320, β_Z=42^g.4140, AB=94.376 m, α_A=161^g.3819, α_B=244^g.7059, ω=244.7059-161.3819=83^g.3240

$\omega+\gamma_D+\beta_D$=199.9980,

(83.3240+7^{cc})+(75.4420+6^{cc})+(41.2320+6^{cc})=200.0000,

$\gamma_{D'}$=75.4426, β_D'=41.2326

3.2.1. Solution with the Classical Method

(AD)=$\gamma_{D'}$, (AZ)=γ_Z, (BD)=200-β_D'=158.7674 (BZ)=200-β_Z=157.5860

AD=$\frac{94.376*sin\beta_D'}{\sin(\gamma_D'+\beta_D')}$=58.95139246 m

BD=$\frac{94.376*sin\gamma_D'}{\sin(\gamma_D'+\beta_D')}$=90.5288754 m

AZ=$\frac{AB*sin\beta Z,}{\sin(\gamma_{Z+\beta_Z})}$=59.8180741 m

BZ=$\frac{AB*sin\gamma_{Z,}}{\sin(\gamma_{Z+\beta_Z})}$=87.4645758 m

$Y_D=Y_A$+AD*sin(AD)=54.61951034 m,

$X_D=X_A$+AD*cos(AD)=22.18052666m

$Y_Z=Y_A$+AZ*sin(AZ)=54.05600204 m,

$X_Z=X_A$+AZ*cos(AZ)=25.61543739 m

ΔY_{DZ}=-0.5635083, ΔX_{DZ}=3.43491073,

(DZ)=389.64825,

DZ=$\sqrt{(\Delta Y_{DZ}^2+\Delta X_{DZ}^2)}$ =3.480826529

φ=(DZ)-(DA)=114.20565,

ψ=(DZ)-(DB)=30.88085

$\alpha_Z=\alpha_A+\varphi$=275.58755, $\alpha_Z=_{AB}+\psi$=275.58675

Average value α_Z=275.58715

3.2.2. Solution with the Second Method

$\beta_Z+\gamma_Z$=114.2420, $\beta_D+\gamma_D$=116.6740, d$\gamma=\gamma_{D'}-\gamma_Z$=3.6146, d$\beta=\beta_Z-\beta_{D'}$=1.1814

b=AZ=$\frac{AB*sin\beta Z,}{\sin(\gamma_{Z+\beta_Z})}$=59.8180741m,

c=BZ=$\frac{AB*sin\gamma_{Z,}}{\sin(\gamma_{Z+\beta_Z})}$=87.46465758m

a=AD=$\frac{AB*sin\beta D\prime}{\sin(\beta_{D\prime}+\gamma_{D\prime})}$ = 58.95139246 mm,

d=BD=$\frac{AB*sin\delta D,}{\sin(\beta_D+\gamma_D)}$=90.5288754 m

DZ=$\sqrt{(a^2+b^2-2*a*b*cosd\gamma)}$ =3.480826518 m

DZ=$\sqrt{(c^2+d-2*c*d*cosd\beta)}$ =3.48082654 m

$\frac{\varphi_1+\psi_1}{2}=\frac{200-d\gamma}{2}$=98.1927,

$\frac{\varphi_1-\psi_1}{2}=arc\tan((a-b)*\tan(\frac{\varphi_1+\psi_1}{2})/(a+b)$=

-16.01295492

φ_1=98.1930+(-16.03904)=82.17974,

ψ_1=98.1930-(-16.03904)=114.20565

$\frac{\varphi_2+\psi_2}{2}=\frac{200-d\beta}{2}$=99.4093,

$\frac{\varphi_2-\psi_2}{2}=arc\tan((c-d)*\tan(\frac{\varphi_2+\psi_2}{2})/(c+d)$=

68.52844

φ_2=99.4090+(-68.50445)=30.88085, ψ_2= 99.4090-(-68.50445)==167.9377

$\alpha_Z=\alpha_A+\psi_1$=275.58755

$\alpha_Z=\alpha_B+\varphi_2$ =275.58675

Average value α_Z=275.58715

3.2.3. Numerical Application 3

In accordance with Figure 1 and Figure 3, calculate the centering elements with the classical method and the second method, taking into account the measurements made at points A, B and D given in Table 3.

Table 3. Measurements made at points A, B and D

Station Point	Point of View	Horizontal Angle	Horizontal Distance	Station Point	Point of View	Horizontal Angle	Horizontal Distance
A	B	0.0000	56.328	D	1	0.0000	
	Z	58.7462			2	138.3164	
	D	60.2465			...		
B	Z	0.0000			A	157.1788	
	D	1.3314			B	231.5709	
	A	66.6934	56.328				

Obtaining and simply balancing the elements to be used in the calculations:

γ_Z=58^g.7462, γ_D=60^g.2465, β_D=65^g.3620, β_Z=66^g.6934, AB=56.328m, α_A=157^g.1788, α_B=231^g.5709, ω=213.5709-157.1788=74^g.3921

$\omega+\gamma_D+\beta_D$=200.0006,

(74.3921-2^{cc})+(60.2465-2^{cc})+(65.3620-2^{cc})=200.0000,

$\gamma_{D'}$=60.2463, β_D'=65.3618

3.3. Solution with the Classical Method

(AD)=$\gamma_{D'}$, (AZ)=γ_Z, (BD)=200-β_D'=134.6382, (BZ)=200-β_Z=133.3066

AD=$\frac{56.328*sin\beta'_D}{\sin(\gamma'_D+\beta'_D)}$=52.37442008m

BD=$\frac{56.328*sin\gamma'_D}{\sin(\gamma'_D+\beta'_D)}$=49.66197913 m

AZ=$\frac{AB*sin\beta Z,}{\sin(\gamma_{Z+\beta_Z})}$=52.96624644m

BZ=$\frac{AB*sin\gamma_{Z,}}{\sin(\gamma_{Z+\beta_Z})}$=48.750235 m

$Y_D=Y_A$+AD*sin(AD)=42.49058137m,

$X_D=X_A$+AD*cos(AD)=30.62075071m

$Y_Z=Y_A$+AZ*sin(AZ)=42.22917398m,

$X_Z=X_A$+AZ*cos(AZ)=31.97061349 m

ΔY_{DZ}=-0.26140739, ΔX_{DZ}=1.34986278, (DZ)=387.8223,

DZ=$\sqrt{(\Delta Y_{DZ}^2+\Delta X_{DZ}^2)}$ =1.374941216

φ=(DZ)-(DA)=127.5760, ψ=(DZ)-(DB)=53.1841

$\alpha_Z=\alpha_A+\varphi$=284.7548,

$\alpha_Z=\alpha_{AB}+\psi$=284.7550

Mean value α_Z=284.7549

3.3.1. Solution with the Second Method

a=AD=$\frac{56.328*sin\beta'_D}{\sin(\gamma'_D+\beta'_D)}$=52.37442008m

d=BD=$\frac{56.328*sin\gamma'_D}{\sin(\gamma'_D+\beta'_D)}$=49.66197913 m

b=AZ=$\frac{AB*sin\beta Z,}{\sin(\gamma_{Z+\beta_Z})}$=52.96624644m

c=BZ=$\frac{AB*sin\gamma_{Z,}}{\sin(\gamma_{Z+\beta_Z})}$=48.750235 m

$d\gamma=\gamma_{D'}-\gamma_Z$=1.5001, $d\beta=\beta_Z-\beta_{D'}$=1.3316

DZ=$\sqrt{(a^2+b^2-2*a*b*cosd\gamma)}$ =1.374941228 m

DZ=$\sqrt{(c^2+d-2*c*d*cosd\beta)}$ =1.374941188 m

$\frac{\varphi_1+\psi_1}{2}=\frac{200-d\gamma}{2}$=99.24995,

$\frac{\varphi_1-\psi_1}{2}=arc\tan((a-b)*\tan(\frac{\varphi_1+\psi_1}{2})/(a+b)=$ -28.32604

φ_1=98.1930+(-16.03904)=70.9239,

ψ_1=98.1930-(-16.03904)=127.5760

$\frac{\varphi_2+\psi_2}{2}=\frac{200-d\beta}{2}$=99.3342,

$\frac{\varphi_2-\psi_2}{2}=arc\tan((c-d)*\tan(\frac{\varphi_2+\psi_2}{2})/(c+d)=$ -46.150109

φ_2=99.4090+(-68.50445)=53.18409, ψ_2= 99.4090-(-68.50445)==145.484309

$\alpha_Z=\alpha_A+\psi_1$=284.7548 $\alpha_Z=\alpha_B+\varphi_2$ =284.7550

Mean value αZ=284.7549

4. EXAMINATION OF NUMERICAL APPLICATION RESULTS

When the results of the centering elements obtained in the above 3.2 and 3.3 numerical applications (Table 4) are examined; It was observed that there was no difference between the elements calculated with the classical method and the second method.

Table 4. Summary of the results of 3.2 and 3.3 numerical applications according to both method

Numerical Application Number	Method Used	Calculation Results of Numerical Applications				
		DZ	$\alpha_Z=\alpha_A+\varphi$	$\alpha_Z=\alpha_B+\psi$	$\alpha_Z=\alpha_A+\psi_1$	$\alpha_Z=\alpha_B+\varphi_2$
2.2	Classic	3.480826	275.58755	275.58675		
	Classic	3.480826			275.58755	275.58675
2.3	Classic	1.374941	284.7548	284.7549		
	Second	1.374941			284.7548	284.7549

5. RESULTS

In the calculation of the centering elements, it is recommended to apply the first method in order to be established from the calculation load. With the electronic tachometer produced today, it is possible to look from one point to another with a certain directional angle. Taking advantage of this feature of the instrument, it is recommended to look at the off-center point, the auxiliary point that enables this point to be marked on the minaret balcony, with a directional angle of 200^g.0000 for ease of calculation in the first method. In this case, the α_Z centering element is 0^g.0000. Numerical applications of centering elements with the classical method and the second method; It was seen that there was no difference between the calculation results and the results were equal to each other. The advantage of the second method is that it does not require coordinate calculation and it can be said that it is equivalent to the classical method in terms of processing load.

Author contributions

The contributions of Yazar1, Yazar2, Yazar3 and Yazar4 to this article is equal.

Conflicts of interest

The authors declare no conflicts of interest.

Statement of Research and Publication Ethics

The authors declare that this study complies with Research and Publication Ethics

REFERENCES

Allan A L, Hollwey J R & Maynes J H B (1968). Pratical Field Surveying and Computations, Heinnemann, London

Atasoy V (2014). Arazi Ölçmeleri, Ekin Basım Yayın Dağıtım, ISBN: 978-605-327-039-3, s.459-470, Bursa

Aydın Ö (1984). Ölçme Bilgisi I, Kurtiş Matbaası, s.59-70, İstanbul

Dilaver A (2010). Jeodezide Sayısal Çözümleme Yöntemleri (Numerik Analiz), KTÜ Harita Müh. Böl., Trabzon

İnce H, Türen Y & Erdem N (2021). Harita Mühendisliği ve Harita Kadastro Teknikerliği İçin Pratik Jeodezik Hesaplar, Nobel Yayını, ISBN:978-625-406-2, s. 264-271

Kıran H (1983). Merkezdışı Gözlemlerin Merkeze Dönüştürülmesi Hakkında Bir Öneri, Harita ve Kad. Müh. Oda Derg, sayı 56-57, s.99-101, Ankara.

Özbenli E & Tüdeş T (1989). Ölçme Bilgisi Pratik Jeodezi, KTÜ Müh. Fak. Yay., s.240-247, Trabzon

Şerbetçi M & Atasoy V (2000). Jeodezik Hesap, KTÜ Müh. Mim. Fak. Yay., s.151-156 Trabzon.

Uren J & Price W F (1986). Surveying for Engineers, Second Edition, ELBS Macmillan, London

URL_1: https://www.sistemas.com.tr (Access date: 04.09.2021)

Yüncü S & Aslan C (2002). Numerik Yöntemlerde Hata Analizi ve Bir Numerik Çözüm Paketinin Hazırlanması, Gazi Ün. Müh. Mim. Fak. Dergisi Cilt 17, No=2, s.87-102, Ankara.

Wolf P R & Ghilani C D (2008). Elementary Surveying an Introduction to Geomatics. 12th Edition, Upper Saddle River, New Jersey: Pearson Prentice-Hall. pp. 233-269

Advanced Geomatics
http://publish.mersin.edu.tr/index.php/geomatics/index

The Brief History of Early Marine-Navigation

Hatice Şeyma Selbesoğlu*[1], Burak Barutçu[2], Aytekin Çökelez[1]

[1]*Istanbul Technical University, Faculty of Science and Letters, Department of Humanities and Social Sciences, Istanbul, Turkey*
[2]*Istanbul Technical University, Energy Institute, Renewable Energy Department, Istanbul, Turkey*

Keywords
Early Navigation
Transportation
Navigational Instrument
Compass
Armillary Sphere
Dead-Reckoning
Nautical Almanac
Ancient Greek
Classics
De Magnete
Eratosthenes

ABSTRACT

This work was supported by Scientific Research Projects Department of Istanbul Technical University. Project Number: 42512. The aim of this study is to examine in the beginnings and development of early navigation systems and to reveal their relationship with disciplines such as astronomy, cartography, horology and map-making. Since prehistoric times, people have been travelling using waterways and highways. Before the transporting by air, oceans was the only way for early intercontinental transportation. Thus, people learned building simple boats to cross seas. As progressing of marine-navigation technologies, the importance of calculating route made it necessary to measure time and distance. Early navigators sailed by observing the celestial bodies such as the sun, moon and stars through the astronomical information. Especially the transition from the earth-centered universe model to heliocentric (Copernican) has astronomically affected the entire early navigation period. Moreover, navigators used early navigation tools such as dead reckoning and cross-staff. And also, they made nautical almanac called ''parapegmata'' in Greek and used primitively designed compasses. Despite all these developments sailors mostly have lost their route due to misinterpreted rotations. Also it has not been easy to make accurate measurements on ships until the eighteenth-nineteenth centuries.

1. HISTORY OF NAVIGATION

Transportation has been necessary since the beginning of human history. Human populations who initially settled near rivers, needed to travel more as their population grows and new settlements are needed. Travelling by road was possible up to limited distance because there were not sufficient highways. In addition, oceans was the only way of the intercontinental travel. Thus, travelling on water could be improved faster. The only thing that matters in the first place was to stay on the water and dry. Human firstly learned how to make raft to cross rivers. But as time passed, people learned to build larger boats and galleys, and it became extremely important to take these vehicles from one point to another. So, the history of navigation has begun. Navigation term etymologically derived from the verb *Navigare*[1], which means traveling in Latin, especially traveling in the sea. Today, the term of navigation, which is used in the sense of travelling on both by sea and on land from one point to another, corresponds to all the meanings of navigation, wayfinding, cruising, shipping and to navigate. It is simplest definition is to determine the most suitable way to go from one point to another or to go from a certain point to another point and to navigate on the most convenient route. Nowadays, while the position of a point on the sea or on land can be easily determined by satellites orbiting the Earth, examining the historical development of navigation from past to present provides a holistic new perspective.

In this context, maps have undoubtedly been one of the most important tools among the primary tools, as well as all kinds of tools and methods such as dead-reckoning, compass, mechanical clock and various observation

[1] Navig/o, are, avi, atum. (Lat.)

* **Corresponding Author**
*(seyma.selbesoglu@itu.edu.tr) ORCID ID 0000-0002-8636-6593
(barutcub @itu.edu.tr) ORCID ID 0000-0002-8834-2317
(cokelez@itu.edu.tr) ORCID ID 0000-0002-8742-3246

Cite this article;
Selbesoğlu H Ş, Barutçu B & Çökelez Aytekin (2021). The Brief History of Early Marine-Navigation. Advanced Geomatics, 1(1), 14-20

Research Article
Received: 06/09/2021; Accepted: 30/09/2021

methods that have been used for navigation directly or as an aid throughout history. One of the most important tools of navigating on the sea are nautical charts in addition to navigational instruments throughout the history. People were able to divide the land they lived on into meaningful pieces thanks to the maps. Major terms such as ''*map*'', ''*charta*'' or ''*karte*'' and ''*mappa mundi*'' stand out in the history of cartography. It is important to separate these terms from each other for reading history. While the map represents maps made in a more general sense, charts in most sources represent nautical charts. It comes from the word - χάρτης (kartes) which means paper in Greek. The term '' *karte*'' was first used in the history of cartography by the German cartographer Laurent Fries. And the map term come from the word ''*mappa*'' in Latin, meaning a napkin, table-napkin or cloth. The term of '' *mappa mundi*''[2] in Late Latin, it may represent the boundaries of the known world of that time, and this *mappa* could contain texts, surveying notes and pictures. The term ''*mappa*'' was used because of them who called *Gromatici* in Latin, recorded drawings and notes of their surveying on cloth, parchment or pieces of *vellum*[3].

2. DEVELOPMENT OF NAVIGATION INSTRUMENTS

The development of technology over time, the distance traveled on the sea has begun to be measured. Primitive measurements on the sea are based on determining time intervals starting from a certain point. Lack of instruments measuring time as we know it today required calculations over time intervals. Instruments such as the hourglass and sundial play an important role in ancient navigation as primitive timers for measuring time over elapsed time. One of the most primitive scientific instruments for measuring time are water clocks called *Clepsydra* (κλεψύδρα)[4] in Greek. Water clocks have been developed to be used at night when the sunlight does not reach the Earth. The most primitive form of water clock is a bowl-shaped outflow form date back to Egypt. One of the most advanced examples of water clocks in ancient times belongs to the famous mechanist and inventor of principles of pneumatic science *Ctesibius* (Fig. 1). The instrument developed by *Ctesibius* also works over time intervals and an alarm system. Knowledge about the primitive water clocks also called *Horologium ex Aqua* in Roman Literature is known through the Roman author, architect and engineer Marcus Vitruvius Pollio's work *''De Architectura Libri Decem*'' written in Latin (Pollio M. V., 2017). In Vitruvius' book, *Ctesibius*'s work on air pressure is mentioned as well as the water clock. *Ctesibius* also put forth the principles of natural air pressure and instruments working with air pressure.

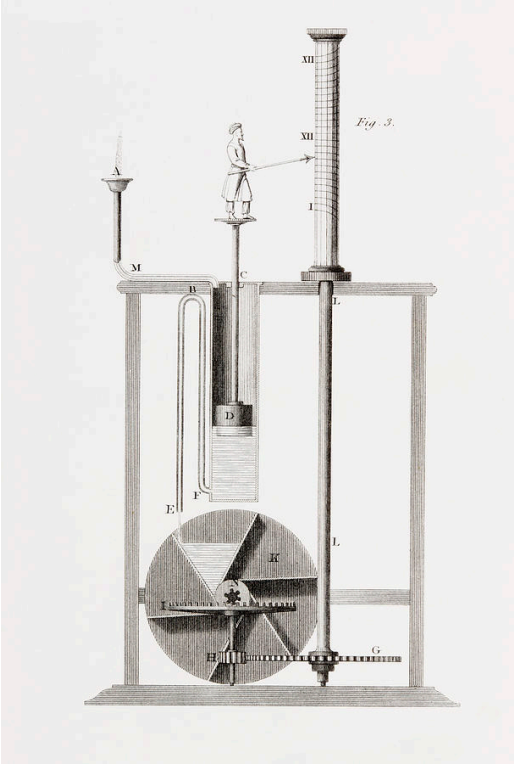

Figure 1. An early 19th century illustration of Ctesibius's clepsydra from the 3rd century BC, the illustrator was probably an English mechanical engineer John Farey Jr. figure in public domain: http://www.antique-horology.org/_editorial/clepsydra/

Measuring certain time periods is not enough for journey on the sea. In order to achieve a useful result, the starting point must be positioned. This is exactly the point that expresses the inseparable part of the history of cartography and navigation. We cannot create a route on the sea without knowing where we are right now. And confirming this thesis, we can witness that mapmaking and navigation technologies are growing simultaneously on the stage of history. It can be said as follows to be more precise: Mapmaking made the development of navigation possible. Besides the science of cartography, astronomy and horology have been the main supporters of navigation science.

With the developing trade and the discovery of new continents, map-making has become more important. From the most primitive symbols and signs used on maps to today's Global Positioning Systems (GPS), the contribution of map making and cartography fields to navigation cannot be disputed.

The oldest known maps are dated to the sixth and seventh centuries BC in the Middle East. Greek geographer Eratosthenes, made one of the earliest scientific world maps. Eratosthenes divided the entire known world according to 5 climate zones. The oldest scientific map of the known world, made by Eratosthenes, covers the from Gibraltar to India and from Somalia to the arctic circle (Fig. 2).

[2] Mundus word could be used to mean the world in Vulgar Latin but that is the meaning of "order" in Latin.

[3] Vellum, i (Lat) : a cloth or calf.

[4] Clepsydra : Water Thief; water-clock, a water-butt with a narrow orifice underneath, through which the water trickled slowly, for measuring periods of time, used to time speeches in the law-courts. (Liddell & Scott, 2009), [κλέπτω (kléptō, "steal") + ὕδωρ (húdōr, "water"].

Towards the end of the third century BC, Eratosthenes was the scientist who reached the closest results to the truth in calculating the circumference of the Earth and the dimensions of known world. It is known that in the second stage, he also benefited from astronomical observations, distance measurements and ship routes on sea (Wright, 1923). Eratosthenes used a special terminology to describe the visual, spatial, epistemic and communicative actions of geography. Therefore, the philology of the language used, Greek, is very important in order to understand and convey the *Geōgraphia* of Eratosthenes (Connors, 2016). In this respect, while the science of geography is examined historically, the fact that philology helps the history of science with a multidisciplinary approach makes it possible to reach the most accurate scientific reality.

He is also the inventor of the geographic coordinate system (GCS). Eratosthenes has determined latitude using stallers and longitude with the lunar eclipse method. GCS is vital in development of sea navigation. Although the science of astronomy emerged and developed in civilizations such as Egypt, Mesopotamia and China, Ancient Greek offers a wider field to research in terms of the abundance of written sources that have survived to the present day. Greek philosophers/scientists[5] travelling to Egypt and China, they learned the science of astronomy and mathematics belonging to that geography and carried it to their hometown. The final step is the transfer of all this knowledge to the west by the Romans and so the historical background of the scientific revolution is almost formed.

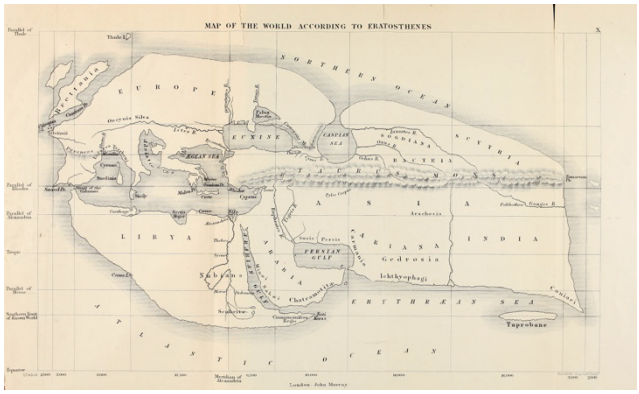

Figure 2. 19th century reconstruction of Eratosthenes' map of the known world. A History of Ancient Geography among the Greeks and Romans from the Earliest Ages till the Fall of the Roman Empire, page 667, London: John Murray, 1883.

The beginning of Ancient Greek Astronomy dates to the Ionian Age. Mesopotamia is rarely mentioned in the Ancient Greek writing sources, but astronomy studies in the Mesopotamian Seleucids era and Ionian age were on the same period. (Unat, 2013). The Greeks who first explained planetary motions with geometric-kinematic systems, were able to describe planetary systems at a level that could explain astronomical phenomena (Unat, 2013). Thus, it did not take long for the μῦθος (myths) and λόγος (*logos*) to separate in Ancient Greek. People used myths and epics for knowledge (getting information, and oral tradition. Information from mythological narratives remained valid even after the emergence of sciences. The term '' *logos* '' (reason) represents scientific thinking. Logos word was used in various meanings.[6] It was used especially by the Sophists and Greek philosopher Heraclitus in the sense of the first power, the first principle in the universe. It was the force that brought order to the primordial chaos. This corresponds to the first people thinking over the epic tradition. In this sense, it represents the cosmic flux in the meaning of a transition from chaos to order corresponds to the human thought which evolving from mythos to the logos phase[7]. Scientific thought and rational knowledge fully formed in Greek created a background that Western science. Greek curiosity (*periergia*)[8] creates the roots of the tree of science. Theories about the cosmology of philosophers can be accepted as the beginning of astronomy in Greek. It has an important role to play in history of astronomy. The image of perfection reached the peak in Ancient Greek and it was accepted and carried to later times, especially through Aristotle's universe and Platonic ideas. The main reason why geocentric universe model which is Ptolemy placed the earth at the center of the universe cannot be rejected is expulsion of human from center of the universe (Fig. 3). This means acceptance of heliocentric universe model (Copernican) (Fig. 4).

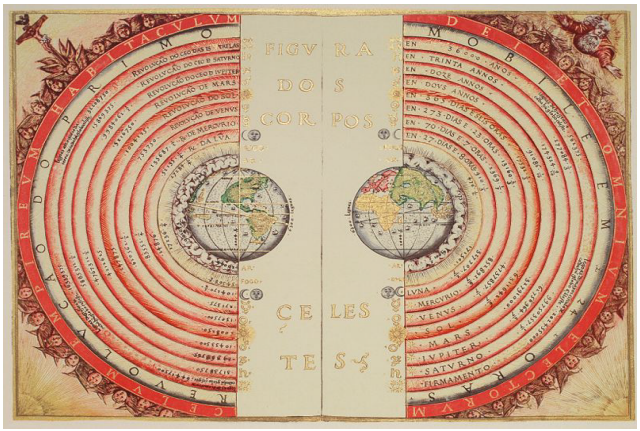

Figure 3. Heavenly bodies from an illustration of the Ptolemaic geocentric (earth-centered cosmography) system by Portuguese cosmographer and cartographer Bartolomeu Velho, 1568, Bibliothèque Nationale, Paris.

[5] φῖλο- (philo-, "beloved, loving") + σοφός (sophós, "wise") – the term of φῖλόσοφος in Ancient Greek includes the title of scientist in today's sense

[6] reason, word,expression

[7] For more reading : Kahn, C. H., Heraclitus, ., & Kahn, C. H. (2004). The art and thought of Heraclitus: An edition of the fragments with translation and commentary. Cambridge [England: Cambridge University Press]., Dürüşken, C., & Bayrak, M. F. (2014). Antikçağ felsefesi: Homeros'tan Augustinus'a bir düşünce serüveni., Gregory, A. (2013). Ancient Greek cosmogony., Laks, A., Most, G. W., Journée, G., Iribarren, L., & Lévystone, D. (2016). *Early Greek philosophy*., In Laks, A., In Most, G. W., In Journée, G., In Lévystone, D., Protagoras, ., Protagoras, ., Gorgias, ., ... Harvard University. (2016). *Early Greek philosophy: Volume VIII, Part 1*.

[8] For more reading: Assmann, J. (2017). Periergia: Egyptian reactions to Greek Curiosity.

Tens of thousands of years ago, peoples sailed across open oceans. More recently, within the past four thousand years, Egyptians and other peoples in the Mediterranean Sea, Persian Gulf, and Indian Ocean dared longer-distance sea travel. Early mariners navigated from island to island by observing the sun and stars, the wind and waves. They noted some objects such as large rocks as guiding points. They observed the behavior of fish and birds. They sailed into the winds, making use of winds that blow east to west just north and south of the equator.

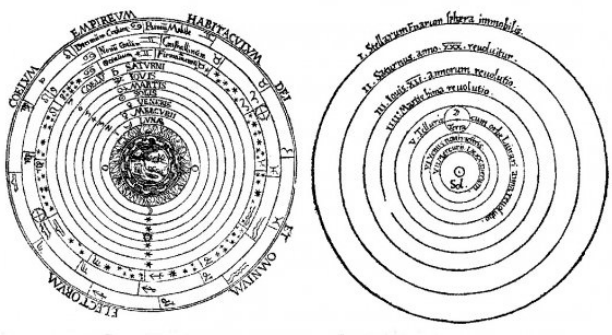

Figure 4. A comparison of the geocentric and heliocentric models of the universe. history.ucsb.edu

The navigation benefitted from the position of the sun with the knowledge of astronomy. Early navigators prepared handbooks of recorded ocean routes and nautical almanacs. Almanac, known as *parapegmata* in Greek, had been composed for centuries. *Parapegmata* or nautical almanacs are the publication describing the cyclical phenomena such as stellar phases, weather, lunar cycles, and more. The Almanacs or *parapegmata* as astronomical diaries, were not enough alone to travel by sea. Therefore, various technological instruments and navigational systems were additionally used.

Dead reckoning is one of the primary and oldest method of marine navigation. It was first developed by Mediterranean navigators. The word *Parakete*, which is the Turkish word of dead reckoning, reflects its etymological origin. It is based on the word *barchetta*, which is thought to have passed from Vulgar Latin[9] to Italian Language (Selbesoğlu, 2021). While the word *barchetto* is mostly used for ships to fishing in the Adriatic Sea, the word *barchetta* is used to describe the wooden piece of dead reckoning instrument (F.Fleck, 2018). The nautical term, which corresponds to the dead reckoning is exactly as *solcometro a bar*chetta in the Italian maritime terminology. This transition of term to the Turkish terminology was realized with the use of the second word, which means small ship.

The oldest dead reckoning chart is *Carta Pisana* dating back to thirteenth century. The oldest surviving nautical chart called *Carta Pisana*, because it was acquired by the Bibliothèque Nationale from a family old-established in Pisa. Dead reckoning that preferred method when celestial observation is unavailable, is a method of navigation relying on estimating one's current position using a previously obtained position. In earlier versions of reckoning, during the cruise, a floating object was thrown into the sea from the fore and the time of this object until it reached the stern of the ship was determined. Then, with the proportionality method, the distance the ship traveled in an hour, in other words its speed was calculated.

In later times, different instruments using properties such as hydrodynamics and electromagnetic, have been made to determine the speed of the ship.

Development of navigation instruments continued throughout the history of ancient maritime. The backstaff is one of them that was used to measure the altitude of a celestial body. Scientific navigational instrument that especially used to measure the altitude of the moon and sun, was invented by English navigator John Davis (Seaman's Secrets in 1594). Therefore backstaff was called Davis quadrant which is the most dominant tool in the history of navigation instruments evolved from the Cross-staff. And Cross-staff also called Jacob's Staff or '' baculum'' (bone) or '' radius'' (staff) in Latin words (Rossi & Russo, 2009).

The Cross-staff, which was originally based on the Greek word βάκλον etymologically, took place in the literature with its Latin version, baculum (Liddell & Scott, 2009). This observational instrument was invented by the astronomer Levi ben Gerson (or Gersonides) who lived in France in the fourteenth century. The Cross-staff instrument is mentioned in Levi ben Gerson's book on astronomy written in Hebrew and translated into Latin while he was still alive. The book, which is one of the most important works written in Hebrew on astronomy in the Middle Ages, contains poems introducing and celebrating the invention of the instrument. In the following parts of the book, Gerson described different versions of cross-staff and explains in detail how to use the instrument (Goldstein & Gerson, 1985, p.155). But Gerson does not make any reference to the use of the Cross-staff in marine-navigation. After Levi ben Gerson, the most detailed descriptions of the Cross-staff in Latin were published in manuscripts dating to the fifteenth century and book that published in 1531 of the mathematician and astronomer Regiomontanus. As He mentioned in his work ''*De cometae magnitudine, longitudineque, ac de loco eius vero problemata XVI*'', the primitive cross-staff basically consists of two parts. Regiomontanus explains that instrument consists of two wooden bars, one movable and one stationary. He used the Latin word *regula*, meaning stick, for the movable rod and used the term *regullela mobilis*[10] for the movable middle part. Although no reference was made in the sources mentioned about the use of navigation, the Cross-staff was widely used by sailors due to its portability (Selbesoğlu, 2021).

Compass also was one of the major instrument for marine navigation. The invention of the compass was made possible by the development of knowledge about magnetism. There are invisible magnetic field lines wrapped around the world. The north and south poles are aligned with the Earth's axis. Thus, magnetic objects

[9] Barca, ae, f (Lat.): small ship, boat, barge. A Latin Dictionary. Founded on Andrews' edition of Freund's Latin dictionary. Revised, enlarged, and in great part rewritten by. Charlton T. Lewis, PhD. and. Charles Short, LLD. Oxford. Clarendon Press. 1879.

[10] This term may have been used to mean a moving little stick.

such as a compass needle or magnetic stone align themselves along a north-south axis (Geary, 1995). The oldest known types of compass work on the principle of the Earth's magnetic property.

Term of ''compass'' etymology derives Latin verb ''*compassare*" (in italian and also may be in Vulgar Latin) combines with ''com'' (with) and the ''*passus*'' (step). In addition to meaning such as measuring with steps, it can be thought to be etymologically related to circular motion because of the name similarity with the drafting compass. The compass as an instrument of navigation and measuring based on stones with magnetic properties. Loadstones which referred to as ''*magnetum*'' in Late Latin writings, made the development of the compass with magnetized needle possible.

Loadstones and their properties were known in Greek. The first known compass is dated to China, during the Han Dynasty (between 2nd c. BC - 2nd c.AD). Chinese realized that the lodestone always points in the same direction when floated in a bowl of water but it isn't unclear whether the Chinese understood that this direction was north, as little was known about global direction finding at that time (Fig. 5). Also, it is not certain that the earliest knowledge about lodestones is dated to China. Fundamental property of the lodestone of attracting iron was certainly known before. The close of the seventh century B.C, loadstones and their magnetic properties were known by the Ancient Greek. Even a legend attributed to the Ida Mountain confirms the existence of information about magnets (the legend of magnes the shepherd).[11] In the texts of many ancient authors such as Thales (640-546 B.C.) and Pliny (23-79 A.D.), the mentions of ''*loadstones*'' were frequently cited. But the first reference to the use of the compass for navigational purposes is found in a Chinese encyclopedia in probably during the Han or Tsin Dynasty. But there was no definite mention of the use of the compass until ''*De Utensilibus*'' written by an English monk, Alexander Neckam. This work occurs in middle ages around the twelfth century (Author, 1919). It became difficult to find the first inventors for advanced compasses (as mariner's compass or advanced magnetic compasses), which spread over many geographies and was developed by different people after the middle Ages and the period of discoveries. Peregrinus is the first that describes the compass with pivoted needle. The first writer to attribute a special knowledge of the compass to the Amalfians was Flavio Biondo, was later cited in other works as the inventor of the mariner compass (Nelson, 1962). The four chief improvements applied to Peregrinus compass in late times: the cap-and-pivot support, the movable fly, the divided needle, and the gimbal suspension (Nelson, 1962). Next developments of compass extend to modern period and technologies developing in time of war.

The first scientists to scientifically reveal the magnetic property of the magnetic stone and Earth magnetism was William Gilbert (1540-1603) in the sixteenth century. He clarified the distinction between electricity and magnetism which until his time were seen as similar principles and also he is regarded as the founder of magnetism as a science. He describes the Earth as a giant magnet. He also has an important place in the history of science and technology, as it was the first to use experimental methods to support his theories. He conducted his magnetic experiments on a instrument that small model of planet Earth which he called the terrella (Fig. 6). This instrument was a spherical magnet like the world Gilbert described. According to William Gilbert, among the known substances, the most similar (element) to that of the Earth is lodestone and iron (Freudenthal, 1983). Gilbert thus paved the way for the development of magnetic science with all these theories and assumptions. In the light of this new approaches, the known cosmology and the relative positions of the planets were also affected by new magnetic science.

Figure 5. Loadstone floated in a bowl of water, Lapis Polaris Magnes, invention of the compass by Flavio Amalfitano (Flavio Gioja or Gioia) in the 1300s from series *Nova Reperta*, Museo Galileo.

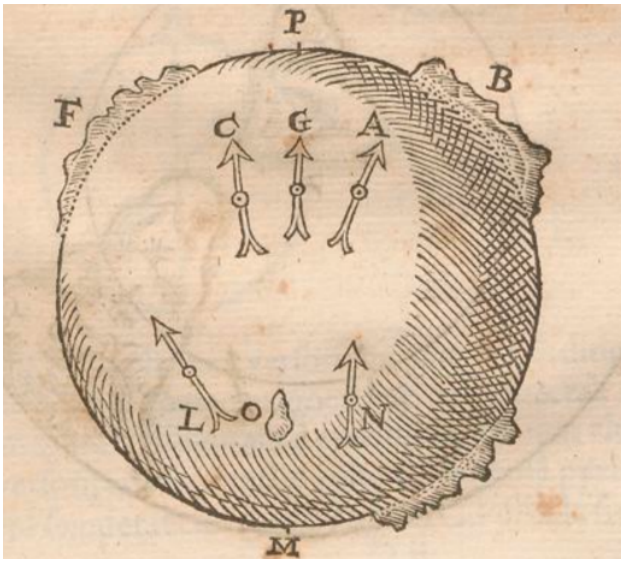

Figure 6. Illustration of small magnetized model ''terrella'' representing the Earth as a giant magnet from Guilielmi Gilberti Colcestrensis, Medici Londinensis, De Magnete, Magneticisque Corporibus et De Magno Magnete Tellure; Physiologia nova, plurimis et argumentis et experimentis demonstrata, 1600, s.157.

[11] It is a legend that describes the discovery of the magnetic property of Mount Ida. (*For more reading: Mourino, M. R. (1991). From Thales to Lauterbur, or from the lodestone to MR imaging: Magnetism and medicine.*)

The compass has been modified for use at sea. The mariner's compass which was invented for this purpose, works on the same principle as the magnetic compass. The mariner's compass, one of the oldest instruments used for navigation is also a type of magnetic compass. Unlike traditional magnetic compasses, it is fixed on the feet in order to remain stable on the ship. It is usually mounted on rings made of brass with the help of joints. Liquids are used in some of the marine compasses in order not to be affected by the movement on the ship. Mostly, a mixture of water and alcohol is used as a liquid. Compass is preserved in wooden or ivory boxes, which are mostly produced to protect the compass. Later, brass material started to be preferred mostly because it caused deviations on the magnetic needle. The use of lead material in the compass needle is also common to make instrument heavy and stable (Selbesoğlu, 2021).

The compass card inside instrument is made of paper material and mostly has a drawing of a compass rose which is a figure used in compasses, nautical charts and some monuments (Fig.8). The figure also called wind rose, has become an important symbol in maritime history and marine-navigation. and There are degrees and direction symbols on the compass card or compass rose. The origin of compass rose or wind rose is thought to be based on the wind classifications in Aristotle's (384-322 B.C) *Meteorologica* work (Fig.7).

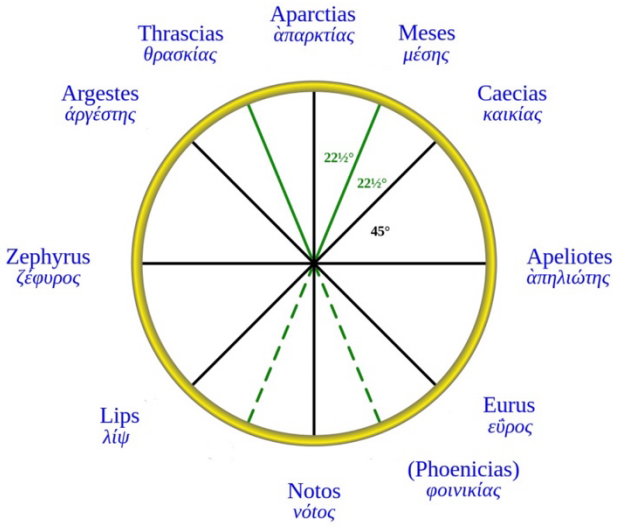

Figure 7. Alternative depiction of the wind rose of Aristotle, on the basis of his *Meteorologica*, illustration from,*https://www.wikiwand.com/en/Classical_compass winds.*

The invention of mariner's compass coincides with the period when Aristotle and his works began to be appreciated again in the Christian world and the translation activities accelerated. Although this relation is not certain, it shows that the markings on the card used in the mariner's compass may have been designed with inspiration from the ancient classification of winds (Taylor, 1951).

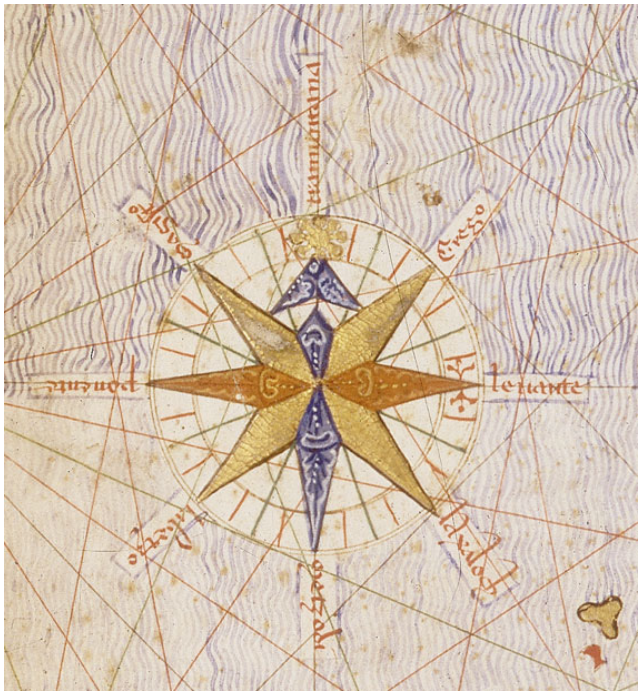

Figure 8. First ornate compass rose depicted on a chart, from the Catalan Atlas (1375), with the Pole Star as north mark from Gallica Digital Library.

3. RESULT

The aim of this study is to examine the beginnings and developments of early navigation instruments and systems and explain how navigation in the sea emerged and developed. Since prehistoric times, people have traveled by using the seas and land routes, and they have struggled to improve their mobility. Before air transportation existed, the only way of intercontinental transportation was to cross the oceans and open seas. This requires advanced ship technology, developed navigational instruments and advanced knowledge of astronomy science. In this way, humanity has made progress in sea transportation with scientific studies in the historical process. With the progress of sea voyage, the importance of route calculation and more precise measurement of time and distances have become necessary. Early sailors laid the foundations of celestial observation by observing celestial bodies such as the sun, moon and fixed stars through their astronomical knowledge. In this context, related astronomical concepts, traditions of thought and primitive navigation instruments such as compass, cross-staff and system of dead-reckoning were especially examined. Lodestones and magnetic science are of great importance, especially for the invention and use of the compass which was a turning point in history of marine-navigation. In this context, the earliest references to loadstones in the literature and the development of magnetic science are emphasized in this study. In addition, information about development and structure of mariner's compass which is a widely used version of the magnetic compass in maritime, is given in the study. The wind rose figure in relation to the compass which forms the basis of card in the mariner's compass also has an important place in maritime history.

Research on instruments only in technical terms does not bring historical integrity. Furthermore, it is not possible to investigate to the history of navigation without examining their relations between other disciplines such as astronomy, cosmology, cartography, horology and map-making. Philology and History sciences help to see all these in a meaningful framework. Also, a whole history of early marine-navigation has been influenced by understandings of the universe, especially during the transition from the earth-centered model of the universe to the heliocentric model. In this connection, various cosmological figures that have changed throughout history have also affected navigation. In addition to the given instruments, there were early instruments that we cannot include in a brief study, used in marine-navigation such as the mariner's quadrant, armillary sphere and astrolabe. These historical navigation instruments will be examined in future studies.

Author contributions

***Hatice Şeyma Selbesoğlu*:** Writing and presenting original draft, writing/manuscript preparation, and commentary, literature search, translation, etymological research of concepts, philological research, scientific preparation, methodology, investigation.

***Burak Barutçu*:** Supervision, validation, access of resources, conceptualization, revision.

***Aytekin Çökelez*:** Project administration, methodology, supervision, validation, access of resources, conceptualization, revision.

Conflicts of interest

The authors declare no conflicts of interest.

Statement of Research and Publication Ethics

The authors declare that this study complies with Research and Publication Ethics

Acknowledgments

This work was supported by Scientific Research Projects Department of Istanbul Technical University. Project Number: 42512. This paper is expanded version of the study presented at the 2nd Intercontinental Geoinformation Days 2021 (IGD) held in Mersin, Türkiye on May 5-6, 2021.

REFERENCES

Author U (1919). Principal Facts of The Earth's Magnetism and Methods of Determining the True Meridian and The Magnetic Declination. (E. JONES, Dü.) Department of Commerce U.S.Coast and Geodetic Survey, Washington.

Bagrow L (1966). History of Cartography. (R. Skelton, Dü.) C.A.Watts & Co, London.

Bunbury E H (1883). A History of Ancient Geography among the Greeks and Romans: from the earliest ages till the fall of the Roman Empire. Published by John Murray, London.

Colcestrensis G G (1600). De magnete, magneticisque corporibus, et de magno magnete tellure. Londini.

Connors C (2016). Eratosthenes, Strabo, and the Geographer's Gaze. Pacific Coast Philology, 46(2), 139-152.

F Fleck H (2018). Dizionario di Nautica e Marineria. (Electronic Resource)

Freudenthal G (1983). Theory of Matter and Cosmology in William Gilbert's De Magnete. ISIS, 74(1), 22-37.

Geary D (1995). Using a map and compass. Mechanicsburg: PA: Stackpole Books.

Johnston A, Connor R, Stephens C & Ceruzzi P (2015). Time and Navigation The Untold Story of Getting from Here to There. (G. McNamee, Dü.) Smithsonian Books, Washington.

Liddell H & Scott R (2009). Greek-English Lexicon. Salt Digitized by the Genealogical Society of Utah, Lake City, Utah.

McLeod A (2016). Astronomy in the Ancient World Early and Modern Views on Celestial Events. Springer International Publishing AG.

Nelson J H (1962). Magnetism of the Earth. U.S. Govt.Print.Off. Washington.

Rossi C & Russo F (2009). Ancient Engineers' Inventions Precursors of the Present. Springer, Milano.

Selbesoğlu, H Ş (2021). Bilim Tarihinde Denizcilik ve Navigasyon, İstanbul Teknik Üniversitesi Lisansüstü Eğitim Enstitüsü, Bilim ve Teknoloji Tarihi Anabilim Dalı, İstanbul.

Unat P (2013). İlkçağlardan Günümüze Astronomi Tarihi. Nobel Akademik Yayıncılık, Ankara (in Turkish).

Pollio, V (2017). De Architectura (Mimarlık Üzerine). (E. Çoraklı, & Ç. Dürüşken, Çev.) Alfa Yayınları, İstanbul.

Taylor, E G R (1951). Early Charts and the Origin of the Compass Rose. The Journal of Navigation, 4(4), 351-356.

Wright, J K (1923). Notes on the Knowledge of Latitudes and Longitudes in the middle ages. ISIS, 5(1), 75-98.

Advanced Geomatics

http://publish.mersin.edu.tr/index.php/geomatics/index

e-ISSN: 2791-8637

Effect of Calibration Point Density on Indoor Positioning Accuracy: A Study Based on Wi-Fi Fingerprinting Method

Behlül Numan Özdemir*[1], Ayhan Ceylan [1]

[1]*Konya Technical University, Faculty of Engineering and Natural Sciences, Geomatics Department, Konya, Turkey*

Keywords
Wi-Fi Positioning
Fingerprinting
IPS
WKNN

ABSTRACT

Indoor positioning refers to all methods used in areas(indoor) where GNSS signals are too weak or non-existent for position determination, using various signals (Signals of Opportunity) and various sensor data. The availability of these signals and sensors for general navigation use is an important factor in terms of cost and feasibility. Considering the diversity of smart mobile devices and the technologies they contain; it is clear that they are perfect candidates for this job. Signals of Opportunity (SoOP) are intended for purposes other than navigation and Wi-Fi is a great example for this. Since majority of mobile devices have built-in Wi-Fi hardware, many studies focused on Wi-Fi positioning. This study used the fingerprint approach, which is among the most successful methods of indoor positioning using this technology. The number of calibration points to be marked in the calibration phase, which is the first of the two stages of this method, affects both the position accuracy and the time and effort spent. In this study, location accuracy was studied using NN, KNN and WKNN algorithms on a radio map with low calibration point density and it was discovered that the NN method provides both simplicity and satisfactory results in all scenarios. It was determined that the mean errors were minimal at the 2-meter point density and better results were obtained with the weighted-KNN algorithm compared to the KNN.

1. INTRODUCTION

The growing usage of smart mobile devices has boosted the demand for indoor location determination significantly. Furthermore, given that individuals spend the majority of their time indoors, this need is growing by the day. Because GNSS signals have yet to fully address this issue, research has concentrated on the use of Signals of Opportunity (Kunhoth et al., 2020). FM waves, Wi-Fi, and Bluetooth are examples of signals whose primary purpose is not navigation. Some of these technologies, which are now accessible in nearly all mobile devices, can be used to determine position indoors. Wi-Fi technology is the most widely used. Several approaches are utilized for determining position using this wireless communication technology (He & Chan, 2016). These are similar to fingerprinting, trilateration, and triangulation. It is unavoidable that the approaches have benefits and drawbacks in comparison to one another. The fingerprint technique, on the other hand, stands out since it does not require any external hardware and can thus be used in any indoor space. (Torres-Sospedra et al., 2015; Wang et al., 2020). Furthermore, the fingerprint technique has gained popularity over signal propagation models since signal propagation is highly variable in an indoor space due to various solid objects and obstacles (Mautz, 2012).

The fingerprint technique relies on a pre-generated radio map of the interior environment, which is a significant drawback. In other words, it necessitates a preliminary investigation that takes time and effort. This pre-study step is known as the Calibration stage, and it is the first of two phases in the fingerprint technique. The other stage is known as the positioning stage. The signal strength information (RSS) received at various points within the building is gathered and saved in a database with the correct location coordinates in the first step. This database is referred to as the radio map described earlier. Each entry in this database is referred to as a fingerprint since it comprises the coordinate information of the point as well as the RSS vector collected from the nearby wireless access points. RSS measurements are performed multiple times at each calibration point due to signal fluctuations. The location is then determined by correlating and comparing RSS measures in this database

* **Corresponding Author**

*(bnozdemir@ktun.edu.tr) ORCID ID 0000-0001-7351-1870
(aceylan@ktun.edu.tr) ORCID ID 0000-0003-4408-4245

Cite this article;

Özdemir B N & Ceylan A (2021). Effect of Calibration Point Density on Indoor Positioning Accuracy: A Study Based on Wi-Fi Fingerprinting Method. Advanced Geomatics, 1(1), 12-26

Research Article

Received: 09/09/2021; Accepted: 30/09/2021

with existing RSS measures. The calibration point with the shortest distance is simply obtained as the current position as a consequence of this procedure, which typically employs the Euclidean distance. While Euclidean signal distance is the most commonly used distance/similarity measure in this comparison, several other distance/similarity measures are also used (Cha, 2007; Torres-Sospedra et al., 2015).

KNN algorithms are employed when the number of calibration points used in this matching is greater than one. In this case, depending on the density of calibration points, the spatial distances and geometry of K selected neighboring points change and this affects the position accuracy. In this study, in order to examine the effect of this, location accuracy was investigated by using different radio maps created by calibration points placed at different densities.

2. METHOD

This study was carried out in the Faculty of Engineering and Natural Sciences building of Konya Technical University (Fig. 1). The wireless network infrastructure of the building consists of approximately 80 wireless access points broadcasting 2.4GHz and 5GHz signals.

Figure 1. Aerial photograph of the building where the application was carried out

The methodology of the study was carried out in the following order.

I. Obtaining and coordinating the CAD plan of the building (Fig. 2)
II. Establishment of calibration points as routes along corridors at desired intervals
III. Conducting coordinated signal strength measurements at each calibration point on the routes prepared with the measurement setup and software (Fig. 4).
IV. Conducting coordinated signal strength measurements at random points to test positioning accuracy
V. Analyzing the collected data with the prepared software

The workflow applied in this study is shown in Fig. 3. Furthermore, the specifics of this procedure are summarized below.

I. Obtaining and coordinating the CAD plan of the building: In order to mark the correct coordinates on the CAD file of the building, it is necessary to make corrections such as scale and rotation of the drawing. This is done with the use of a total station instrument and a few basic typical terrestrial observations.

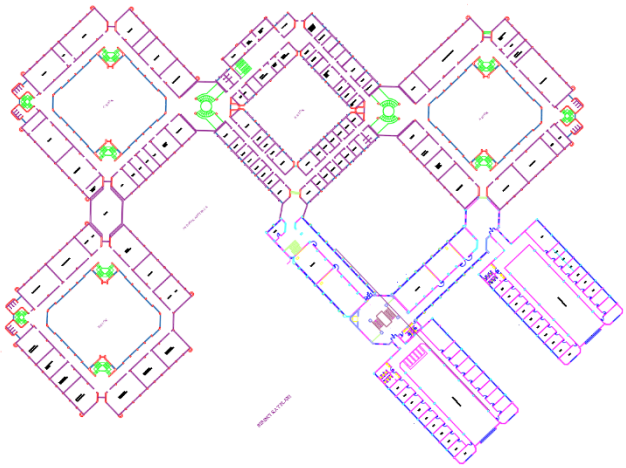

Figure 2. CAD plan of the building

II. Establishment of calibration points as routes along corridors at desired intervals: After the first step, every point to be marked on the CAD will have the actual coordinate. Taking advantage of this, points were placed at equal intervals on the routes created along the corridors. Thus, it has become possible to make high-accuracy calibration measurements by moving along the route from the starting point. With the method we have put forward, the measurement at the calibration points by following the routes has accelerated this stage.

III. Conducting coordinated signal strength measurements at each calibration point on the routes prepared with the measurement setup and software: The signal strength measurements were completed with the measurement setup by importing the coordinate list of these marked points into the mobile data collection software. With this software, information such as the number of measurements at the point where RSS measurement will be made, signal frequency (2.4GHz-5GHz), coarse GNSS coordinates can be recorded.

In this stage, the operator monitors the distance traveled along the route from the screen on the measuring wheel and starts the measurement from the mobile device when the relevant point is reached. The Δs correction between the axis on which the measuring tool makes the length measurement and the axis on which the mobile device makes the RSS measurement has been applied to all measurements (Fig. 4).

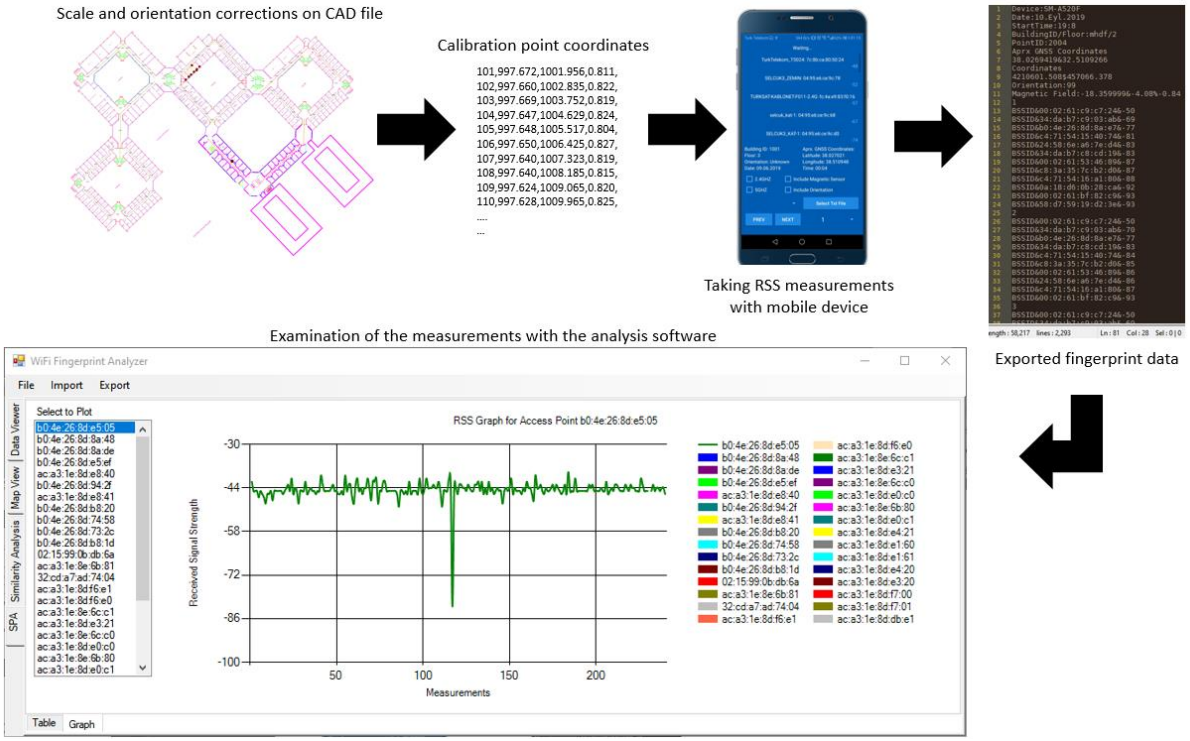

Figure 3. Workflow implemented in the study

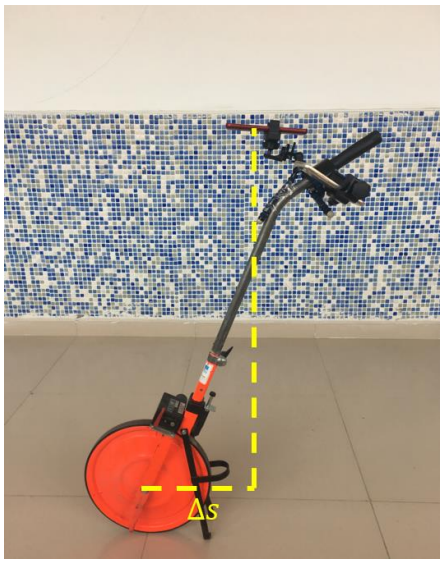

Figure 4. Measurement setup consisting a measuring wheel and a mobile data collection device

Wireless signals propagating indoors are subject to some fluctuation (Jooyoung Kim et al., 2016). This is due to both the hardware in the wireless access point emitting the signal, the hardware of the mobile device receiving these signals, and the variable indoor environmental conditions (Fig. 5). For this reason, in studies, multiple RSS measures are usually made at a calibration point and the average of these measures is used.

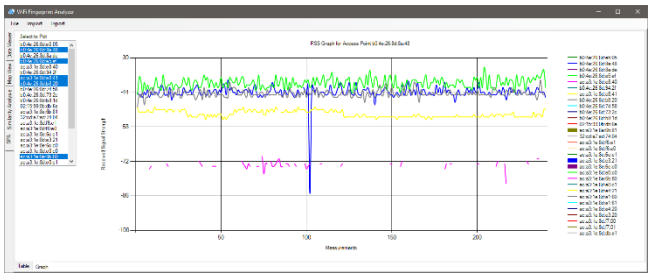

Figure 5. An example of signal fluctuation

Although there is no specific number in the studies on the subject, the number of measurements between 5-20 is generally preferred in terms of time-accuracy. We utilized a database of three observations at each calibration point in this work to decrease the influence of signal variations and experiment with a quicker calibration phase.

To determine the point positioning accuracy, measurements were taken at 237 test points and 1771 calibration points. In addition, the table below shows the number of calibration points for data arranged between 1 to 5 meters to investigate the effect of various neighbor numbers/calibration point density (Table 1).

Table 1. Point densities

Gap between two calibration points	Total Calibration Points
1 m	1771
2 m	907
3 m	606
4 m	471
5 m	366

IV. Conducting coordinated signal strength measurements at random points to test positioning accuracy: In order to test the location accuracy of the system, coordinated RSS measurements were also carried out at various random points.

V. Analyzing the collected data with the prepared software: A program based on .NET and coded in C# was used to quickly evaluate the data obtained in various scenarios. A summary of the features of the program is given in section 2.2.

2.1. Position Estimation

The performance of the fingerprinting varies depending on the number and density of calibration points. In addition, the positioning algorithm also affects the results. These factors should be taken into account and analyzed during the positioning phase. Therefore, we tested the performance of NN and k-NN algorithms at various calibration point densities.

The k-Nearest Neighbor rule compares a current sample to all the labelled samples from a database (Cover & Hart, 1967). It's a distance-based classifier that necessitates the creation of a database for comparisons in which all of the samples are appropriately labeled (Torres-Sospedra et al., 2015). Euclidean distance is often used as the base metric in these comparisons. The Euclidean distance which is used to determine similarity is calculated as (1), where P and Q are two signal vectors and j is the vector length.

$$d_{euclidean}(P,Q) = \sqrt{\sum_{i=1}^{j} |P_i - Q_i|^2} \quad (1)$$

While the nearest neighbor algorithm selects the calibration point with the shortest Euclidean distance, the k-KNN algorithm chooses the K closest calibration points and calculates the position as the mean of their X and Y coordinates (2).

$$P(X,Y) = \frac{1}{K}\sum_{i=1}^{K}(x_i, y_i) \quad (2)$$

Because the impact of each neighbor on the point is evaluated equally in this technique, a certain degree of inaccuracy is introduced (Fig. 6).

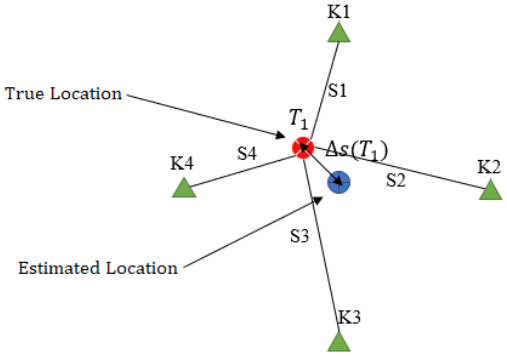

Figure 6. Error caused by means in the KNN algorithm

By prioritizing nearby points in accordance to their Euclidean distances, the WKNN algorithm mitigates the problem's impact (3).

$$w_i = \frac{1/D_i}{\sum_{j=1}^{k} 1/D_j} \quad i = 1,2,\dots,k \quad (3)$$

2.2. Analysis Software

The results of the tests were evaluated using the Wi-Fi fingerprint location program that we created. The following are the program's main features:

- Thresholding to remove WAPs under certain signal strength
- Plotting signal strength changes over time
- Viewing calibration points on the map
- Interpolation module
- Position estimation with weighted measurements
- Analyzing with Euclidean, Manhattan, Minkowski L3-5 and Sørensen distances
- Different data representation schemes (dBm, Exponential Function and Powed (Torres-Sospedra et al., 2015), Positive, Normalized and Experimental Functions)

3. RESULTS and DISCUSSIONS

When the number of neighbors selected in the KNN algorithm rose beyond two, the average inaccuracy increased by up to six meters. As the reason for this, we can say that with the increasing number of neighbors, more irrelevant points have affected the location determination. In this case, the weighted KNN algorithm provides a reduction in maximum errors by distributing relative weights to distant points (Fig. 7). This is especially true in corridor-style interior areas. However, in hall-type interior environments where the number of relevant nearby calibration point counts is significantly larger, this situation might give quite different results (Shin et al., 2012).

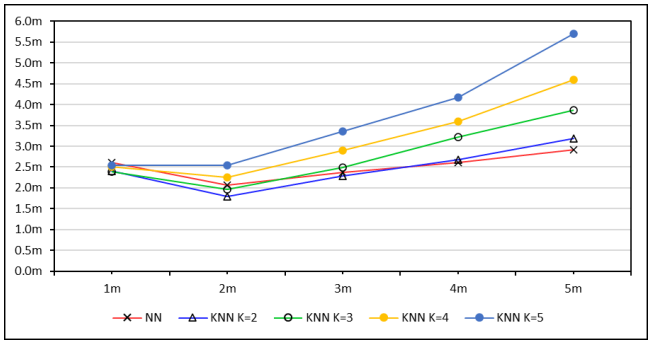

Figure 7. Mean errors of KNN with different neighbor numbers and calibration point gaps

The WKNN method, which has lower average errors, provides comparable results (Fig. 8). WKNN is more successful in this case since it reduces the impact of insignificant points on position estimation.

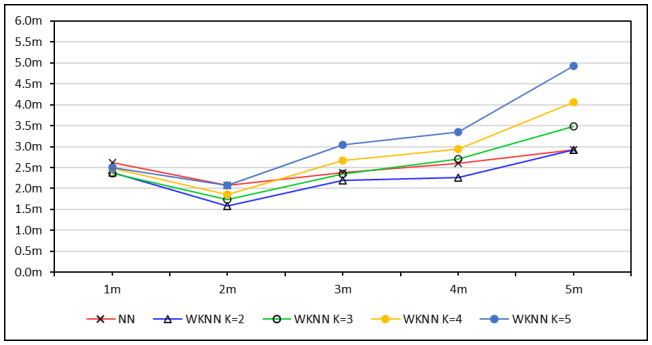

Figure 8. Mean errors of WKNN with different neighbor numbers and calibration point gaps

When each case is examined separately to determine the optimal point spacing, the 2-meter distribution has the lowest mean errors. Distributions of 1- and 3-meter intervals produced the best outcomes in second place (Fig. 9-10-11-12). As seen in Figures 9 and 10, all three methods up to three neighbors produced fairly similar results. It is also evident that the NN algorithm provides reasonable results in all ranges, particularly those greater than 3 meters.

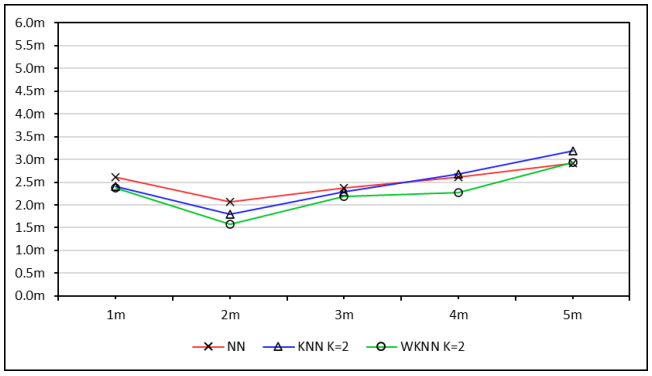

Figure 9. Mean errors of different neighbor numbers for each algorithm, K=2

The total number of test points and their placements are obviously related to the performance of the NN algorithm, which yields comparable average errors at intervals bigger than 3 meters. Because the distance between consecutive calibration points is large in a corridor type indoor environment, we can claim that the nearest calibration point to a location in that corridor will be equal to or closer to the specified interval.

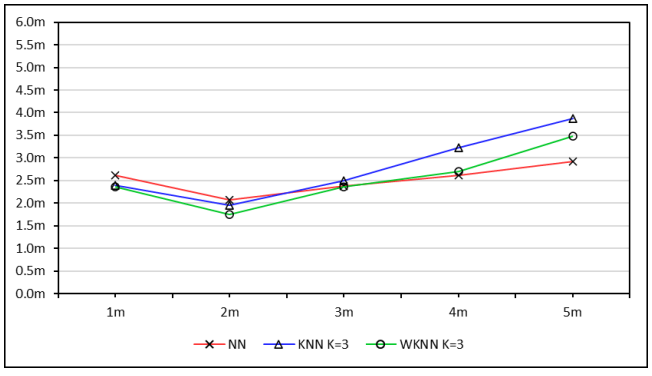

Figure 10. Mean errors of different neighbor numbers for each algorithm, K=3

When the number of neighbors exceeds 3, it is seen that the difference between KNN and WKNN widens, which is an expected result (Fig. 11-12).

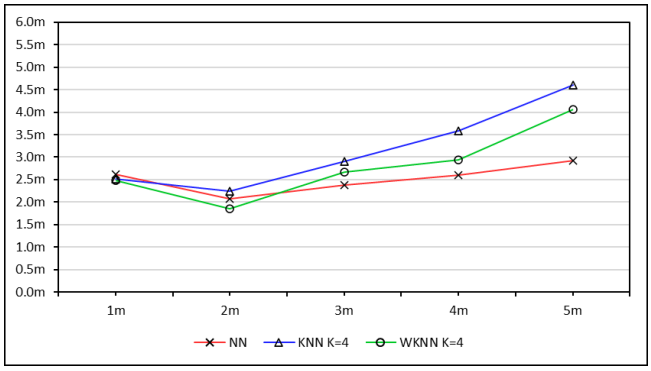

Figure 11. Mean errors of different neighbor numbers for each algorithm, K=4

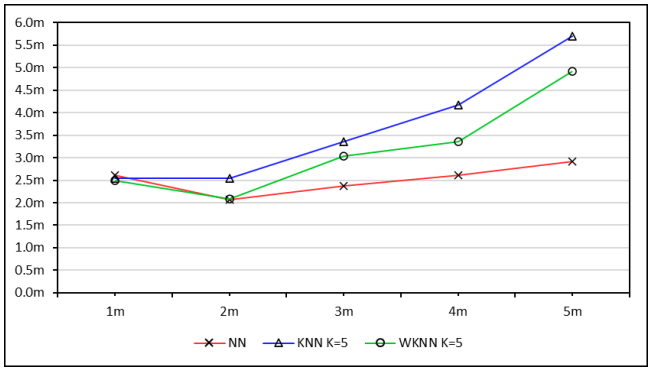

Figure 12. Mean errors of different neighbor numbers for each algorithm, K=5

Tables 1 and 2 also show the standard deviations generated from each scenario. In the NN-KNN comparison, the lowest standard deviation was obtained at K=2 and K=3 cases, while in WKNN this situation was realized at K=3 and K=5 cases.

Table 2. Standard deviations of NN and KNN algorithms

Gap between two calibration point	NN	KNN K=2	KNN K=3	KNN K=4	KNN K=5
1 m	2.45	2.33	2.22	2.34	2.29
2 m	2.38	1.79	1.70	1.80	1.87
3 m	2.16	2.05	1.70	2.17	2.27
4 m	2.71	2.20	2.40	2.61	2.85
5 m	2.42	2.76	2.65	3.11	3.52

Table 3. Standard deviations of NN and WKNN algorithms

Gap between two calibration point	NN	WKNN K=2	WKNN K=3	WKNN K=4	WKNN K=5
1 m	2.45	2.32	2.21	2.31	2.25
2 m	2.38	1.81	1.65	1.81	1.79
3 m	2.16	2.01	1.64	1.99	2.09
4 m	2.71	2.19	2.23	2.40	2.53
5 m	2.42	2.62	2.39	2.75	3.18

4. CONCLUSION

We offered a comparative analysis of fingerprint matching methods for Wi-Fi RSS signal-based indoor localization systems in this work. In terms of localization errors, the proposed study compares the performance of the NN, KNN, and WKNN fingerprint matching algorithms. The experiment was carried out in a real indoor environment, and the experimental results showed that the three positioning algorithms produced different results in different scenarios. Although the NN algorithm produced stable results for each scenario in terms of location accuracy compared to the other two, it is seen that its success is lower when the standard deviations are examined.

Creating a radio map requires careful planning, but determining an appropriate grid density is difficult. It is very important to find the optimum calibration point density as the time and effort spent will increase as the point density increases. It also has an effect on position accuracy. In our study area, the best density was determined as 2 meters. Since this parameter depends on the floor plan and the locations and number of available APs, it needs to be analyzed separately for different indoor spaces.

In addition, it has been observed that the location accuracy decreases as the number of selected neighbors increases. Although this is connected to the geometry of the interior area (Corridor-Type) and a fixed K-value(Bi et al., 2018), dynamic K-value algorithms can offer superior outcomes in a variety of circumstances. This will be the first topic we test in our next research.

Moreover, it would be interesting to investigate the effect of the number of access points and the number of RSS measurements made at each point on location accuracy.

ACKNOWLEDGEMENT

This study was produced from the doctoral thesis named "RSS Based Indoor Positioning Approach in Indoor Environments: Implementation of Fingerprinting Method and Its Performance Analysis" and is an expanded version of the paper presented orally at the " 2nd Intercontinental Geoinformation Days (IGD)" conference.

Author contributions

Behlül Numan Özdemir: Conceptualization, Methodology, Software, Data curation, Writing-Original draft preparation, Software, Validation
Ayhan Ceylan: Visualization, Investigation, Writing-Reviewing and Editing.

Conflicts of interest

The authors declare no conflicts of interest.

Statement of Research and Publication Ethics

The authors declare that this study complies with Research and Publication Ethics

REFERENCES

Bi J, Wang Y, Li X, Qi H, Cao H & Xu S (2018). An Adaptive Weighted KNN Positioning Method Based on Omnidirectional Fingerprint Database and Twice Affinity Propagation Clustering. Sensors, 18(8), 2502. https://doi.org/10.3390/s18082502

Cha, S.-H. (2007). Comprehensive Survey on Distance/Similarity Measures between Probability Density Functions. 1(4), 8.

Cover T & Hart P (1967). Nearest neighbor pattern classification. IEEE Transactions on Information Theory, 13(1), 21–27. https://doi.org/10.1109/TIT.1967.1053964

He S & Chan S.-H. G. (2016). Wi-Fi Fingerprint-Based Indoor Positioning: Recent Advances and Comparisons. IEEE Communications Surveys & Tutorials, 18(1), 466–490. https://doi.org/10.1109/COMST.2015.2464084

Jooyoung Kim, Myungin Ji, Ju-il Jeon, Sangjoon Park & Cho Y (2016). K-NN based positioning performance estimation for fingerprinting localization. 2016 Eighth International Conference on Ubiquitous and Future Networks (ICUFN), 468–470. https://doi.org/10.1109/ICUFN.2016.7537073

Kunhoth J, Karkar A, Al-Maadeed S & Al-Ali A (2020). Indoor positioning and wayfinding systems: A survey. Human-Centric Computing and Information Sciences, 10(1), 18. https://doi.org/10.1186/s13673-020-00222-0

Mautz R (2012). Indoor positioning technologies [Application/pdf]. 1 Band. https://doi.org/10.3929/ETHZ-A-007313554

Shin B, Lee J H, Lee T & Kim H S (2012). Enhanced Weighted K-Nearest Neighbor Algorithm for Indoor Wi-Fi Positioning Systems. International Journal of Networked Computing and Advanced Information Management, 2(2), 15–21. https://doi.org/10.4156/ijncm.vol2.issue2.2

Torres-Sospedra J, Montoliu R, Trilles S, Belmonte Ó & Huerta J (2015). Comprehensive analysis of distance and similarity measures for Wi-Fi fingerprinting indoor positioning systems. Expert Systems with Applications, 42(23), 9263–9278. https://doi.org/10.1016/j.eswa.2015.08.013

Wang B, Gan X, Liu X, Yu B, Jia R, Huang L & Jia H (2020). A Novel Weighted KNN Algorithm Based on RSS Similarity and Position Distance for Wi-Fi Fingerprint Positioning. IEEE Access, 8, 30591–30602. https://doi.org/10.1109/ACCESS.2020.2973212

Advanced Geomatics

http://publish.mersin.edu.tr/index.php/geomatics/index

e-ISSN: 2791-8637

Housing Valuation Model in Samsun, Atakum District with Artificial Neural Networks and Multiple Regression Analysis

Mehmet Emin Tabar*[1], Aslan Cihat Başara [2], Yasemin Şişman [3]

[1]*Bitlis Eren University, Vocational School of Technical Sciences, Department of Architecture and Urban Planning, Bitlis, Turkey*
[2]*Ondokuz Mayis University, Institute of Graduate Studies, Department of Geomatics Engineering, Samsun, Turkey*
[3]*Ondokuz Mayis University, Faculty of Engineering, Department of Geomatics Engineering, Samsun, Turkey*

Keywords
Real estate appraisal
Multiple regression analysis
Artificial neural network
Artificial intelligence
Matlab

ABSTRACT

Valuation, in its simplest form, is the determination of the amount that a property will be processed at a certain date. Valuation can be done for many purposes. These; can be listed as buying and selling, transfer, tax assessment, expropriation, inheritance distribution, investment, financing and credit. There are various methods of valuation. These methods are examined under 3 main groups as traditional, statistical and modern valuation methods. The aim of the article is to provide an overview of regression analysis, one of the statistical valuation methods, and artificial neural networks, one of the modern valuation methods, and to compare the accuracy values. Matlab software was used for artificial neural network modeling and Minitab software was used for regression analysis. The accuracies of the obtained values were determined by the average absolute percent error (MAPE) formula.

1. INTRODUCTION

Real estate is independent and permanent rights registered on a separate page in the land register and independent parts of the property ownership register. Also, real estate gives owners the right to use as she wishes, except for the restrictions developed for the benefit of the public. (Açlar and Çağdaş 2002). Real estate valuation and these values reflection as tax are the most important economic foundations of developed societies. The real estate market has gained a positive momentum with the development of real estate investment trusts, construction companies, education, technology and professionalism. These developments have also brought professional real estate appraisals to the agenda in order to make the right investments (Atik et al. 2015). The house is the place where the consumer lives with families. (Özdamar 2004). The valuation process can be defined as determine the value of something measured with money. In this process, the attributes of something are valuated (Yomralıoğlu et al. 2011). Real estate valuation is made for trading or corporate transactions that varies according to needs, wishes and financial capacity. (Ring and Dasso 1977). According to another definition, it is the process of determining the provision of the seller according to the properties of the property for investment or long-term use (Brown 1965). Real estate valuation is done in many different ways. However, for professional real estate valuation, a mathematical model should be mentioned rather than subjective value estimates (Tabar and Şişman 2020). In traditional valuation methods, valuation experts try to make value calculations by only estimating an exchange price. Thus, the traditional methods are far from being objective compared to statistical and modern valuation methods since they do not depend on a mathematical model. Statistical and modern methods involve less initiative as they depend on a mathematical model. The most important issues in the valuation area is the need to that the information provided to the customer is clear. (Pagourtzi et al. 2003). When the methods used in the mathematical model are examined; many methods such as fuzzy logic, artificial neural networks, spatial analysis, support vector machines, regression analysis are reached. The most used real estate valuation methods are shown in Table 1.

* **Corresponding Author**

*(metabar@beu.edu.tr) ORCID ID 0000 – 0002 – 3234 – 5340
(aslancihatbasara@gmail.com) ORCID ID 0000 – 0001 – 6644 – 6097
(ysisman@omu.edu.tr) ORCID ID 0000 – 0002 – 6600 – 0623

Cite this article;

Tabar M E, Basara A C & Sisman Y (2021). Housing Valuation Model in Samsun, Atakum District with Artificial Neural Networks and Multiple Regression Analysis. Advanced Geomatics, 1(1), 27-32

Research Article

Received: 04/09/2021; Accepted: 30/09/2021

Table 1. The most used real estate valuation methods

Traditional methods	Statistical methods	Modern methods
Comparison method	Nominal method	Fuzzy logic
Income method	Multiple regression method	Artificial neural networks
Cost method	Hedonic pricing method	Support vector machine

In this study, multiple regression analysis, one of the statistical valuation methods, and artificial neural networks, one of the modern valuation methods, were used. Accuracy of methods were calculated with the formula of average absolute percent error (MAPE). The comparison was made according to the MAPE of methods.

2. MATERIAL AND METHOD

2.1. Material

Atakum district is one of the most important and most preferred districts in Samsun in terms of real estate valuation. Atakum is listed as the 23rd district in the most housing sales ranking among 923 districts of Turkey in 2019. A total of 10607 housing properties were sold in Atakum in 2019. This study in Samsun, Yenimahalle Neighborhood, a real estate valuation model was created using artificial neural networks and multiple regression analysis and the value was estimated. The study area is shown in Fig 1.

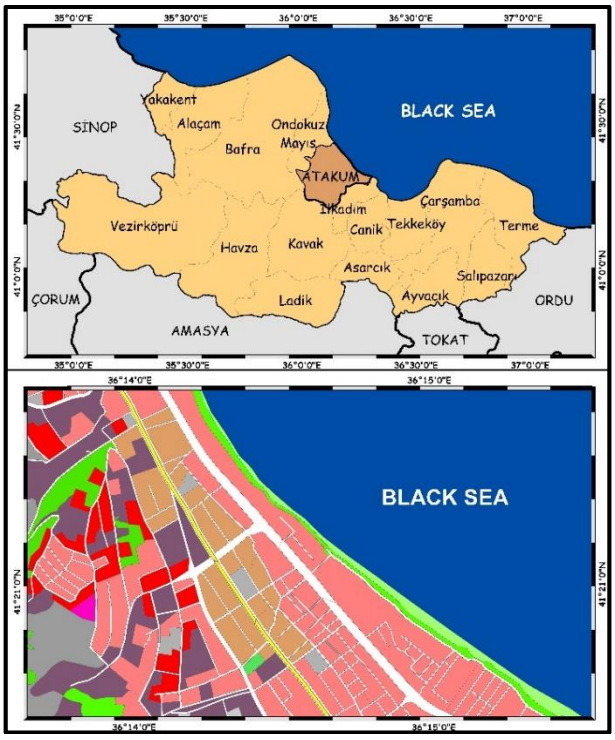

Figure 1. Study area

The data were obtained from a housing sales site. While choosing the housing, care was taken to choose those with a facade to the tramway street. Housing prices are valid from August to October 2020. Housing prices were determined by modeling the obtained data with multiple regression analysis and artificial neural networks. Minitab software was used for this process. The estimated values after modeling were compared with the housing values.

2.2. Method

2.2.1. Multiple Regression Analysis

Multiple regression analysis consists of response and independent variables. The number of response variables is single, but the number of arguments can be more than one. The relationship between response and independent variables can be defined as linear curvilinear exponential etc., If there is only one independent variable and the relationship is linear, it is called simple linear regression, if there are two or more independent variables and the relationship is linear, it is called multiple linear regression. In regression analysis, it is aimed to make the relationship between variables functionally meaningful and explain this relationship with a model (Chatterjee and Hadi 2015).

In valuation models, more than one variable can be combined to form a variable. These variables can also affect each other. Therefore, single regression analysis is not possible. More than one analysis using variables is called multiple regression analysis (Karacabey and Gökgöz 2012). In multiple regression, there are more than one independent variable affecting the response variable. These types of studies have two general purposes:

- Which of the independent variables or finding out which ones affect the response variable more.
- Response variable with the help of independent variables estimate.

The mathematical model of the regression method is as follows:

$$Y_i = \beta_0 + \beta_1 X_{1i} + \beta_2 X_{2i} + \ldots\ldots\ldots + \beta_n X_{ni} + \varepsilon$$

Yi: response variable
Xi: independent variable
i = 1, 2, ..., n

β_0: Returns the value of the point where the line intersects the y-axis. It takes names like intercept.

β_i: It is the slope of the line. It takes names such as slope, speed, regression coefficient (Durmuş 2016).

The result of the regression analysis is tested with some values as determination and correlation coefficient. The determination coefficient is named as the R^2 (Sisman 2014). The R^2 indicates the goodness of fit for the model (Sisman et al. 2014). The R^2 value is a measure of linearity. The range of R^2 is between 0 and +1. If R^2 value is close to +1, the observation values means it's dispersing around the line (Efe et al. 2000). The correlation coefficient is indicating the relationship between two statistically. The range of correlation coefficient is between -1 and +1. If the correlation coefficient is" 0 ", there is no relationship between X and Y. Also, If the correlation coefficient is close to " +1 or -1 " there is positive or negative relationship between X and Y (Güngör and Sevindir 2013).

2.2.2. Artificial Neural Networks

Artificial neural networks emerged by artificially imitating the way the human brain works. It can be thought of as a complex system that occurs as a result of connecting many nerve cells in the brain with different levels of influence. In artificial neural networks, the system first performs the learning process by analyzing input data and output data (Öztürk and Şahin 2018). It gives approximate outputs of new input data after learning process as a result of iterations. Artificial neural networks are especially used in engineering applications. Engineering problems that are difficult to solve with classical methods have gained a different dimension with artificial neural networks and have created an effective alternative (Yegnanarayana 2009). Although the human brain is limited in mathematical operations such as division, multiplication, addition, subtraction, it is more successful than machines in many processes such as learning, remembering, and predicting. The main features of artificial neural networks are nonlinearity, learning, parallel working, generalization, working with missing data, using a large number of variables and parameters, applicability, fault tolerance and flexibility.

Artificial neural networks consist of 3 main components. These; architectural structure, learning algorithm and activation function. When we examine the architectural structure, the input layer consists of the hidden layer and the output layer. In the learning algorithm, the weights in the whole network should take optimal values. In fact, training the net is to find the best value of the weights (Graupe 2013). The activation function provides the match between input and output layers.

Artificial neural networks learn by making mistakes. Basically, artificial neural networks learn in 3 stages. In the first step, outputs are calculated. In the second step, it compares the outputs with the target outputs and calculates the error. In the last stage, the process repeats by changing the weights (Livingstone 2008). Architecture of multilayer artificial neural network is shown in Fig 2 as input layer, hidden layer and output layer.

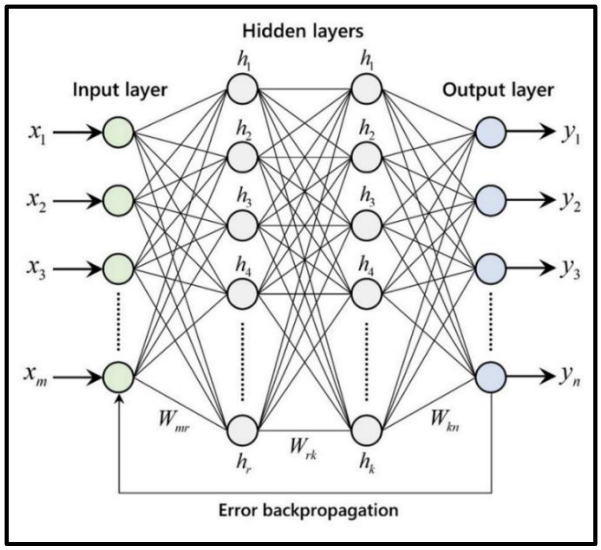

Figure 2. Architecture of multilayer artificial neural network (Fernández-Cabán et al. 2018)

Artificial neural networks consist of multi-layer computational units. The data received from the external environment is applied to the input layer and processed at the entrance, the information is transmitted to the middle layer without any change in the flow direction. The information entering the process in these layers is transmitted forward to the output layer. Artificial neural networks based on the working principle of transmitting information in the forward direction from input to output are called forward feed artificial neural networks (Canan 2006).

3. APPLICATION AND RESULTS

In Samsun, Atakum, Yenimahalle Neighborhood, 200 data were collected about the properties and values of the houses facing the tramway. Housing data are generally shown in Table 2.

Table 2. Housing data

Area	Number of rooms	Building age (Years)	Floor/Number of floors	Number of bathrooms	Balcony	Furnished	Value (TRY)
45	1+1	0	0/4	1	Yes	Yes	205 000
125	3+1	21-25	0/4	2	Yes	No	300 000
160	4+1	11-15	8/8	2	Yes	No	375 000
85	2+1	0	-1/4	1	Yes	No	260 000
130	3+1	5-10	5/8	2	Yes	No	435 000
…	…	…	…	…	…	…	…
130	3+1	4	1/5	1	Yes	No	349 000
145	3+1	0	1/6	2	Yes	No	475 000
135	3+1	0	1/6	2	Yes	No	495 000
145	3+1	16-20	6/6	1	Yes	No	290 000
95	2+1	11-15	0/7	2	Yes	Yes	260 000

These values were transformed into tables and normalized with maximum minimum normalization.

$$Normalized\ data = \frac{(x - \min)}{max - min}$$

For the multiple regression analysis, the normalized data were defined in Minitab program. The result of the analysis was taken as a mathematical model and compared with the actual values of the test data. For the artificial neural network analysis, the artificial neural network module in Matlab software was used. The normalized housing data were defined as input, output and test data. A feed forward network was created using this module. For the test data, the outputs of the Matlab software are taken and compared with the real housing values.

A comparison was made by calculating the accuracy of models using MAPE.

$$MAPE = 100\frac{\sum_{i=1}^{n}\frac{|A_i - F_i|}{A_i}}{n}$$

In this formula, A_i is the real value and F_i is the predicted value.

3.1. Multiple Regression Analysis Application

Normalized housing variables were defined in Minitab software and regression equation was obtained. Housing values were obtained as follows;

Housing Value = (-0.612 + 0.405 area + 0.307 room + 0.4227 b.age + 0.1027 floor + 0.1712 bathroom + 0.2276 balcony - 0.0229 furnished)

The calculated normalized value has been converted into the real house value with the maximum-minimum formula.

Normal probability plot created according to the value of the house is shown in Fig 3.

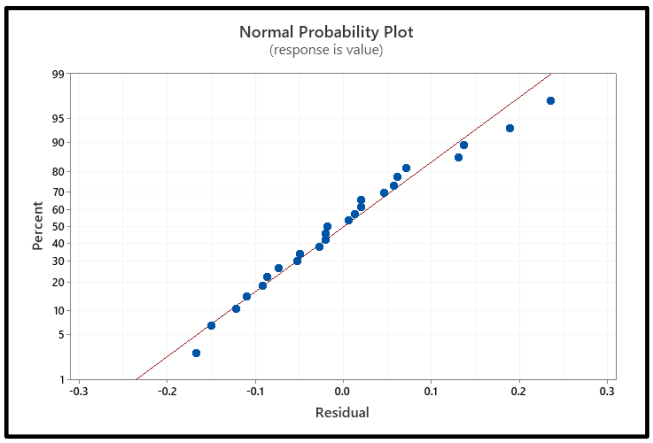

Figure 3. Normal probability plot

The values calculated by multiple regression analysis are shown in Table 3 together with the housing sale prices.

Table 3. Multiple regression analysis results

MRA Value (TRY)	Sale Value (TRY)	Accuracy (%)
219361.667	205000.000	92.994
294014.667	300000.000	98.004
410175.000	375000.000	90.620
286537.000	260000.000	89.793
380271.000	435000.000	87.418
...	...	...
331190.000	349000.000	94.896
437010.667	475000.000	92.002
426800.667	495000.000	86.222
295148.667	290000.000	98.224
267976.333	260000.000	96.932

3.2. Artificial Neural Networks Application

Normalized housing data are defined in Matlab software. The training of the network was carried out with 8 neurons using experimental data with the created feed forward artificial neural network. The training process was repeated a few times to make the learning process more accurate. The maximum failure value was entered as 500, and the iteration amount was determined as 1000.

The accuracy and consistency values of the data were examined by looking at the regression chart after the training. The trained network is simulated with test data.

Housing values were determined by applying the maximum-minimum normalization reversed to the values obtained. Artificial neural network training regression is shown in Fig 4. The results are shown in Table 4.

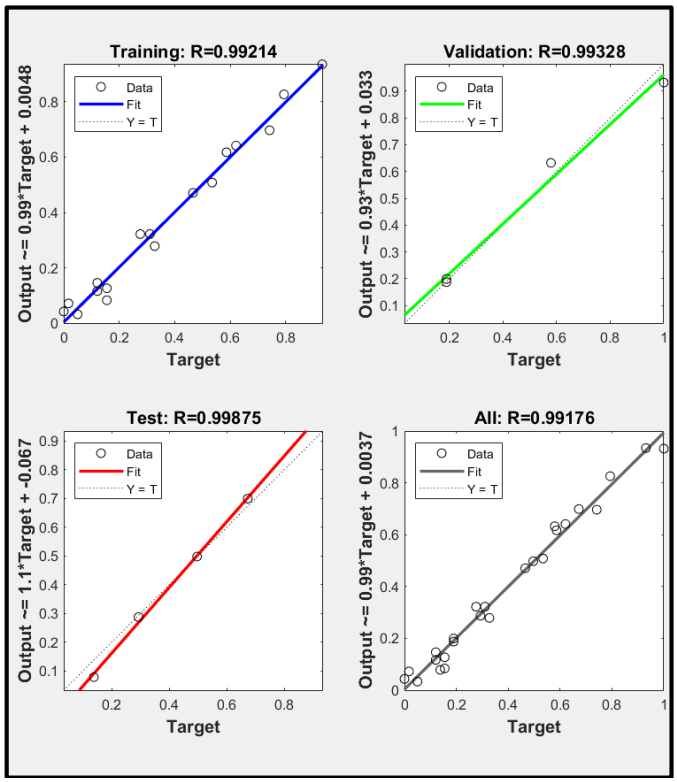

Figure 4. Artificial neural network training regression

Table 4. Artificial neural network results

ANN Value (TRY)	Sale Value (TRY)	Accuracy (%)
222862.080	205000.000	91.286
293771.863	300000.000	97.923
376021.579	375000.000	99.727
257108.193	260000.000	98.887
454902.955	435000.000	95.424
...	...	...
320026.201	349000.000	91.698
471619.035	475000.000	99.288
471124.399	495000.000	95.177
291098.107	290000.000	99.621
259925.188	260000.000	99.971

4. DISCUSSION

In the study, the values obtained in the housing valuation model created using multiple regression analysis and artificial neural networks were compared with the real values of the houses and the accuracy of methods were determined. The housing data was taken used in the study were obtained from Samsun province Atakum district Yenimahalle neighborhood. In determining the housing, the ones facing the tramway street were chosen as the location.

The total accuracy value obtained in the multiple regression analysis was determined as 93.232%. The total accuracy value obtained in artificial neural networks was determined as 97.090%.

5. CONCLUSION

Considering the accuracy values obtained in the study, it is seen that the housing valuation model created with artificial neural networks gives a higher accuracy value. Multiple regression analysis is more suitable in terms of ease of application and understandability of the model. In artificial neural networks, there may be some results that vary with the change of the number of neurons and the selection of functions. The authors recommend the use of statistics and modern methods in frequent applications such as real estate appraisal.

Author contributions

1st Author: Conceptualization, Methodology, Software, Data Curation, Writing-Original Draft Preparation, Validation, Visualization
2nd Author: Visualization, Data Curation
3rd Author: Investigation, Reviewing and Editing

Conflicts of interest

The authors declare no conflicts of interest.

Statement of Research and Publication Ethics

The authors declare that this study complies with Research and Publication Ethics

REFERENCES

Açlar A & Çağdaş V (2002). Taşınmaz (gayrimenkul) değerlemesi. TMMOB Harita ve Kadastro Mühendisleri Odası, Ankara.

Atik M, Köse Y, Yilmaz B & Erbaş M (2015). Şehirlerin İlerleme Yönlerinin Gayrimenkul Değerleri Üzerindeki Etkisinin Ölçülmesi. Çankırı Karatekin Üniversitesi, 5, 443-458.

Brown R K (1965). Real estate economics: an introduction to urban land use: Houghton Mifflin.

Canan S (2006). Yapay sinir ağları ile GPS destekli navigasyon sistemi. Selçuk Üniversitesi Fen Bilimleri Enstitüsü.

Chatterjee S & Hadi A S (2015). Regression analysis by example: John Wiley & Sons.

Durmuş B (2016). Konut Fiyatlarını Etkileyen Parametrelerin Çoklu Regresyon Analizi Yöntemiyle İrdelenmesi Ve Kentsel Dönüşüme Katkıları. Fen Bilimleri Enstitüsü.

Efe E, Bek Y & Şahin M (2000). SPSS'te Çözümleri ile İstatistik Yöntemler II, Kahramanmaraş Sütçü İmam Üniversitesi Rektörlüğü Yayın No: 73, Ders Kitapları Yayın No: 9, KS Ü. Basımevi, Kahramanmaraş, 214.

Fernández-Cabán P L, Masters F J & Phillips B M (2018). Predicting roof pressures on a low-rise structure from freestream turbulence using artificial neural networks. Frontiers in Built Environment, 4, 68.

Graupe D (2013). Principles of artificial neural networks (Vol. 7): World Scientific.

Güngör A & Sevindir H C (2013). Isparta İlindeki Atmosferde Bulunan Kükürt dioksit (SO2) ve Partikül Madde (PM) Konsantrasyonunun Çoklu Doğrusal Regresyon Yöntemi İle Modellenmesi. Journal of Natural and Applied Science, 17(1), 95-108.

Karacabey A & Gökgöz F (2012). Çoklu Regresyon Modeli. Anova Tablosu, Matrislerle Regresyon Çözümlemesi, Regresyon Katsayılarının Yorumu.

Livingstone D J (2008). Artificial neural networks: methods and applications: Springer.

Özdamar N (2004). 4822 Sayılı Yasa İle Değişik 4077 Sayılı Yasa'da Tanımlanan Konut Nedir. Türkiye Barolar Birliği Dergisi, Yıl, 17, 317-331.

Öztürk K & Şahin M E (2018). Yapay Sinir Ağları ve Yapay Zekâ'ya Genel Bir Bakış. Takvim-i Vekayî, 6(2), 25-36.

Pagourtzi E, Assimakopoulos V, Hatzichristos T & French, N (2003). Real estate appraisal: a review of valuation methods. Journal of Property Investment & Finance.

Ring A A & Dasso J J (1977). Real estate principles and practices: Prentice Hall.

Sisman Y (2014). The optimization of GPS positioning using response surface methodology. Arabian Journal of Geosciences, 7(3), 1223-1231.

Sisman Y, Elevli S & Sisman A (2014). A statistical analysis of GPS positioning using experimental design. Acta Geodaetica et Geophysica, 49(3), 343-355.

Tabar M E & Şişman Y (2020). Bulanık Mantık ile Arsa Değerleme Modelinin Oluşturulması. Türkiye Arazi Yönetimi Dergisi, 2(1), 18-24.

Yegnanarayana B (2009). Artificial neural networks: PHI Learning Pvt. Ltd.

Yomralıoğlu T, Nişancı R Çete, M & Candaş E (2011). Dünya'da ve Türkiye'de Taşınmaz Değerlemesi.